Use of Azimuthal Square-Array Direct-Current Resistivity to Locate a Geologic Structure at Fort Detrick, Maryland

by Dorothy H. Tepper and Daniel J. Phelan

BLANK

CONTENTS

FIGURES

FIGURES - Continued

TABLES

APPENDIX

CONVERSION FACTORS AND VERTICAL DATUM

Multiply	By	To obtain
meter (m)	3.281	foot
kilometer (km)	0.6214	mile

Vertical datum: In this report, "sea level" refers to the National Geodetic Vertical Datum of 1929—a geodetic datum derived from a general adjustment of the first-order level nets of the United States and Canada, formerly called Sea Level Datum of 1929.

Use of Azimuthal Square-Array Direct-Current Resistivity to Locate a Geologic Structure at Fort Detrick, Maryland

By Dorothy H. Tepper and Daniel J. Phelan

Abstract

This report presents the results of the azimuthal square-array direct-current resistivity surveys performed by the U.S. Geological Survey at Fort Detrick in Frederick, Maryland, from July 8 through 13, 1998. The purpose of this investigation was to determine if there was geophysical evidence of a suspected geologic structure crossing Area B near the eastern base boundary. If this structure is present, there is some concern that contaminants may be migrating along it. If so, this structure might provide an ideal site to install an extraction well to intercept contaminants before they can migrate beyond the base boundary.

The report includes a discussion of the following topics: geologic setting, the square-array direct-current resistivity method, methods used to perform the surveys, and results and interpretation of the surveys. A total of four profiles and three soundings were performed. Because resistivity along two of the profiles showed little change and was probably affected by buried debris, these profiles were not interpreted. Soundings were interpreted on the basis of graphical results and results from the software program FITELLIPSE.

The area where the resistivity surveys were performed was selected because it is within 0.4 kilometers of the intersection of an earlier mapped fault trending 131 degrees with a fault trending 66 degrees. A fault or unconformity also has been mapped in this area by the U.S. Army Corps of Engineers and in an earlier study. In addition, the field site is adjacent to the base boundary near Robinson Spring.

The data from the profiles and soundings are consistent with the presence of a fault (or unconformity) that trends 66 degrees between two of the soundings. In addition, a calculated trend of 71–77 degrees or the offset on the anomalies on two profiles is consistent with the 66 degree trend. On the basis of some assumptions concerning the actual depth of the soundings, the dip of the fault would range from 6.7 to 13.3 degrees, which is relatively close to the dip of 20 degrees estimated in an earlier study on the unconformity.

Introduction

A suspected geologic structure crosses Area B near the eastern boundary of Fort Detrick, near Frederick, Maryland (figs. 1 and 2). If this structure is present, there is some concern that ground-water contaminants may be migrating along it. If so, this structure might provide an ideal site to install an extraction well to intercept contaminants before they can migrate beyond the base boundary. The U.S. Geological Survey (USGS), in cooperation with the Baltimore District of the U.S. Army Corps of Engineers, performed azimuthal square-array direct-current (d.c.) resistivity surveys at Fort Detrick from July 8 through 13, 1998, to determine if there was geophysical evidence of the suspected structure.

Purpose and Scope

This report presents the results of the azimuthal square-array d.c. resistivity surveys performed by the USGS at Fort Detrick from July 8 through 13, 1998. The azimuthal square-array d.c. resistivity technique was used to answer the following questions:

• What is the fracture orientation in the near-surface bedrock?

• Is there an apparent change in fracture orientation in the near-surface bedrock and with depth?

• Is there evidence of a geologic structure on the basis of changes in primary and secondary fracture orientations?

• If a structure is present, can preliminary information on its depth be determined?

• If a structure is present, how closely can it be located?

The report includes a discussion of the following topics: geologic setting, the square-array d.c. resistivity method, methods used to perform the surveys, and results and interpretation of the surveys.

Description of the Field Site

The area where square-array d.c. resistivity profiles 1-4 and soundings 1-3 (fig. 1) were performed was selected because it is near the intersection of faults trending 66° (degrees) and 131° that were mapped by Jonas and Stose (1938) (fig. 2). A fault or unconformity also has been mapped in this area by the U.S. Army Corps of Engineers (1983) and ICF Kaiser Engineers (1998). In addition, the field site is adjacent to the base boundary near Robinson Spring (fig. 1). Because the area is an open grassy field with minimal cultural interferences such as powerlines or buried utilities, it was suitable for working with the electrodes and electrical cables necessary for this geophysical technique. A utility check determined that a polyvinyl chloride (PVC) gas pipeline is buried along the shoulder of the road, but no other buried utilities are in the area. Building demolition debris is reportedly buried along the southernmost extent of profiles 2 and 4 according to the base personnel performing the utilities checks.

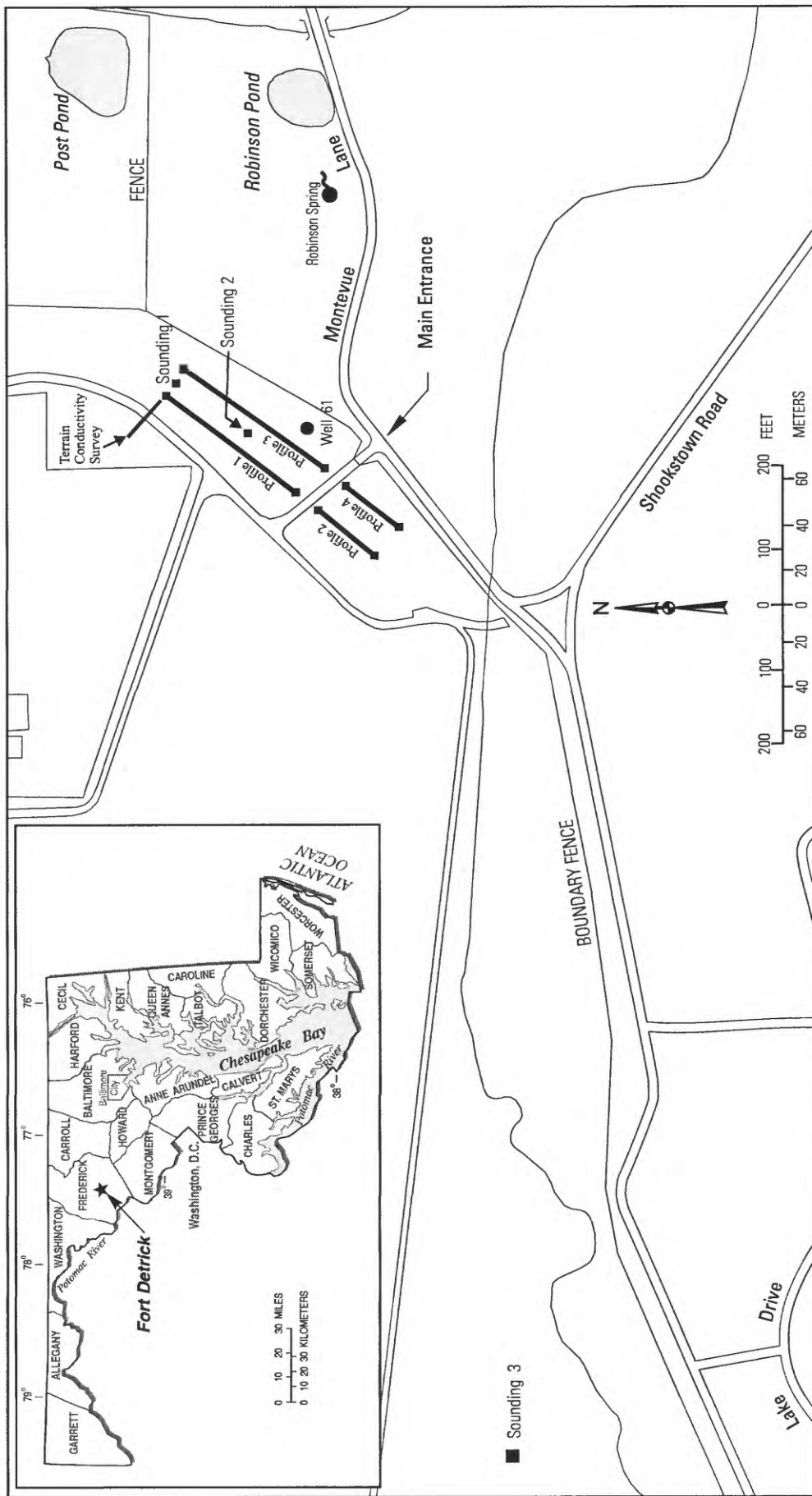Figure 1. Location of Fort Detrick, Frederick, Maryland, and locations of the square-array direct-current resistivity profiles 1-4 and soundings 1- 3 (modified from ICF Kaiser Engineers, 1998).
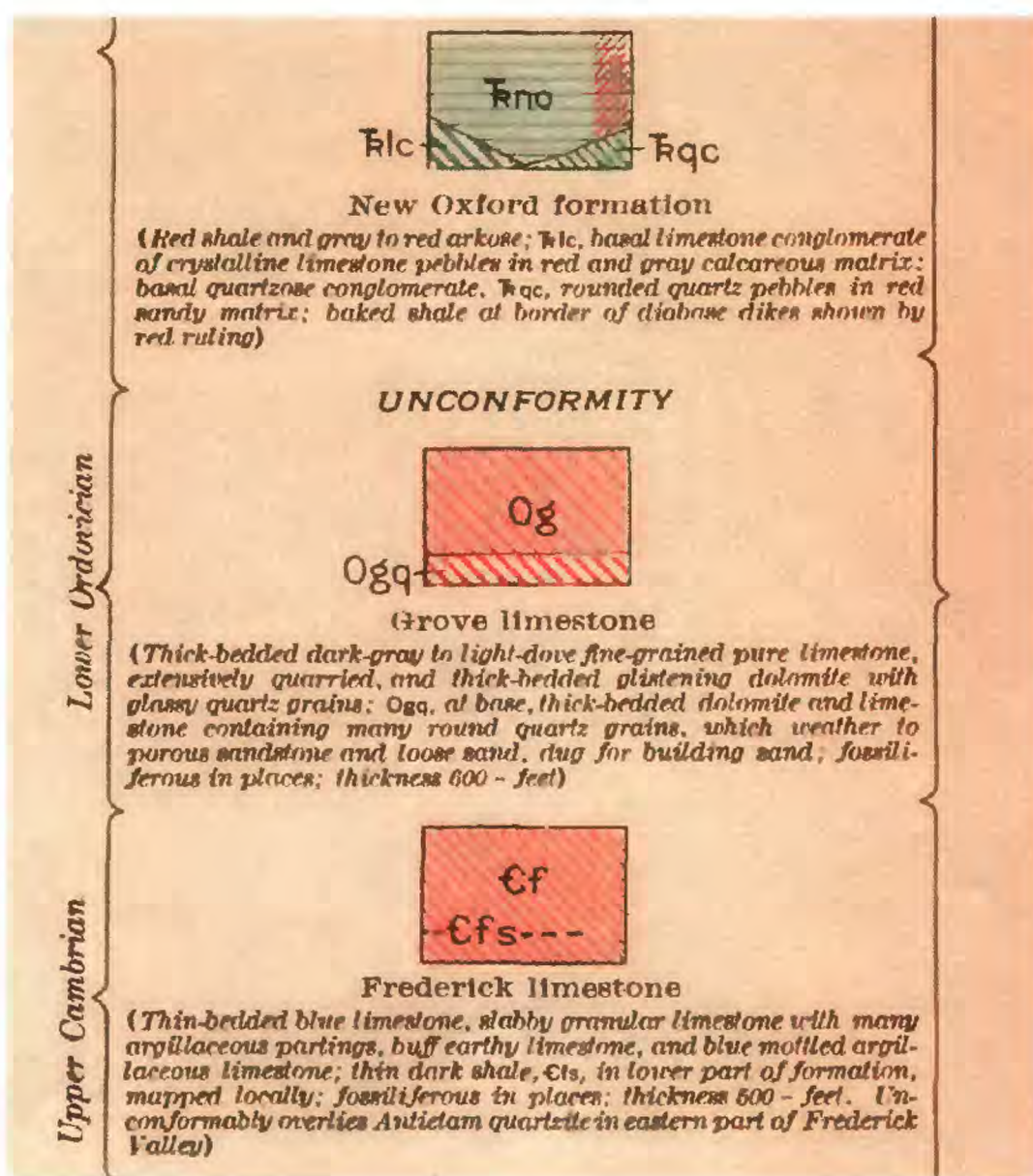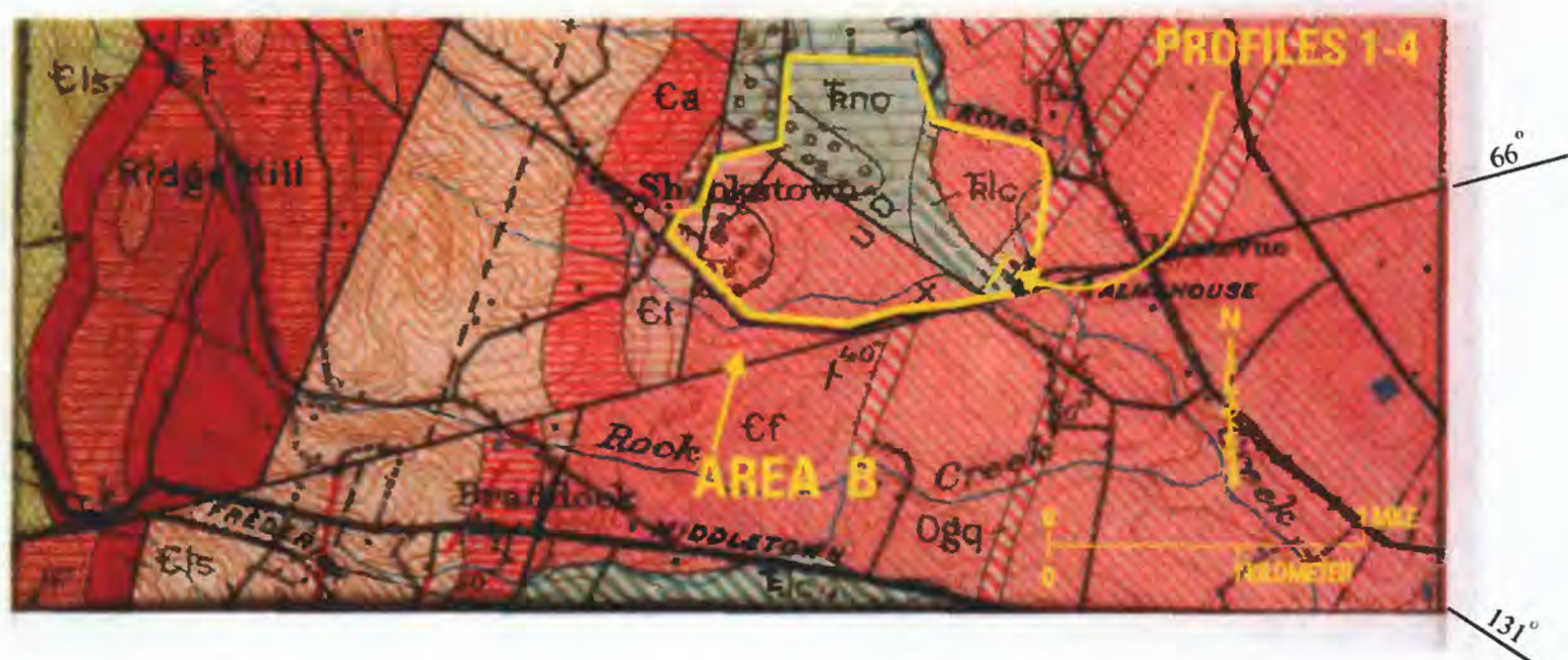
3

Figure 2. Geologic map and lithologic descriptions for the vicinity of Area B, Ft. Detrick, Maryland (from Jonas and Stose, 1938). Faults trending 66° and 131° are identified in the margin of the geologic map.

Geologic Setting

Fort Detrick is near the western edge of the Piedmont Physiographic Province, which is characterized by rolling topography. An early geologic map of Frederick County was produced by Jonas and Stose (1938). The Frederick County part of the State geologic map (Cleaves and others, 1968) and revisions of other mappers were included in a report by Duigon and Dine (1987, plate 1). Fort Detrick lies within the north-south trending Frederick Valley, which is underlain primarily by the Frederick and Grove Limestones (fig. 2).

Stratigraphy The Frederick Limestone (Upper Cambrian) is a dark gray, thin-bedded, argillaceous limestone that contains numerous small fractures filled with secondary calcite, and the total stratigraphic thickness is about 150 m (meters) (Nutter, 1973). The Upper Cambrian and Lower Ordovician Grove Limestone, which is approximately 180 m thick, is a thick-bedded, nearly pure limestone with massive beds of fine-grained dolomite in the lower part and highly quartzose limestone at the base (Nutter, 1973).

The Paleozoic rocks are overlain by Triassic sediments that include conglomerates, sandstones, siltstones, and shales. The Triassic New Oxford Formation, which crops out in the Fort Detrick area (fig. 2), overlies Paleozoic rocks in the western and northern parts of the Frederick Valley and to the south in Virginia (Reinhardt, 1974). The New Oxford Formation includes a basal limestone conglomerate member consisting of limestone pebbles and cobbles in a fine-grained matrix containing quartz grains (Nutter, 1973). This basal conglomerate can be mistaken for the Frederick Limestone in areas where the limestone clasts are predominant and where little or no matrix material is present. It grades to a quartz-pebble conglomerate north of Frederick (Jonas and Stose, 1938). The Frederick Valley apparently was once completely covered by Triassic sedimentary rocks (Nutter, 1973).

The following discussion of the stratigraphy at Area B is condensed from the Draft Remedial Investigation Report for Area B (ICF Kaiser Engineers, 1998, p. 2-4 - 2-5). The Rocky Springs Member of the Frederick Limestone underlies the southern part of Area B. The strike is approximately 35° and the dip is to the southeast at approximately 50°. The Rocky Springs Member in this area is a thin-bedded argillaceous limestone with numerous calcite-filled fractures. Solution cavities frequently were encountered at depths ranging from 3 to 57 m bls (below land surface). In the northern part of Area B, the Rocky Springs Member is unconformably overlain by the Triassic New Oxford Formation. According to Nutter (1973), the New Oxford Formation near Area B strikes approximately 35° and dips 20° to the northwest; however, this unit is thought to be an alluvial fan deposit and as such, does not have true strike and dip. Although this formation contains conglomerate, shale, sandstone, and siltstone, the northern part of Area B primarily is underlain by the conglomerate and there is a small area of shale, sandstone, and siltstone in the northwestern section. Solution cavities up to 5 m long have been encountered at depths ranging from 5 to 52 m bls in the New Oxford Formation.

Structural Geology The Triassic rocks in Carroll and Frederick Counties typically strike northeast and dip to the northwest at an average of 20°, but the dip ranges from 5° to 40° (Nutter, 1975). Of the three predominant joint sets in the Triassic rocks of the Frederick Valley, the most predominant set consists of joints that parallel the strike and are steeply dipping; joint sets that

strike 315° and 300° and that dip steeply to the east are somewhat less prominent; and a joint set that strikes east-west is least prominent (Nutter, 1975).

The Frederick Valley is an asymmetrical synclinorium that is bounded on the west by Catoctin Mountain (Reinhardt, 1974), which is a limb of the South Mountain Anticlinorium (Cloos, 1941, 1947; Whitaker, 1955). The western edge of the valley is formed by a Triassic high-angle reverse fault (Nutter, 1973). The Frederick Valley is bordered on the east by the Martic Line, which separates the phyllites of the western Piedmont from the rocks of the Frederick Valley (Reinhardt, 1974). Jonas and Stose (1938) mapped a fault that separates the Frederick Limestone (Cambrian) from conglomerates of the Triassic New Oxford Formation. The fault offsets several Cambrian stratigraphic units, beginning approximately 1.6 km (kilometers) southwest of the site, with the area of offset continuing more than 3.5 km farther to the southwest along the fault. Cambrian and Precambrian units are offset along this fault to the northeast, beginning approximately 8.8 km northeast of the site. A fault with the same general orientation and position as the one mapped by Jonas and Stose (1938) is shown in Nutter (1975), but is not discussed in that report. That fault offsets the Triassic border fault along Catoctin Mountain and extends eastward across the Frederick Valley at a trend of approximately 77°.

The field site is near the faults trending 66° and 131° that were mapped by Jonas and Stose (1938) and is within 0.4 km of the mapped intersection of these faults. ICF Kaiser Engineers (1998, p. 2-5 and Exhibit 2-4) does not mention these faults, but instead refers to an unconformity in Area B that separates the Triassic New Oxford conglomerates from the Cambrian Frederick Limestone. Because the unconformity was interpreted to be a zone of higher permeability, ICF Kaiser Engineers (1998) mapped its surface trace on the basis of surface-drainage features. This trace corresponds in shape to the area on the Jonas and Stose (1938) map where the Triassic New Oxford conglomerate is truncated near the intersection of the faults trending 66° and 131° (fig. 2). The true dip of the unconformity is estimated by ICF Kaiser Engineers (1998) to be about 20°, which corresponds to the dip of the Triassic rocks (20° to the northwest, according to Nutter, 1973) that were deposited on the surface of the unconformity. In the area where the resistivity profiles were run, the unconformity shown by ICF Kaiser Engineers (1998) is most likely related to the faults mapped by Jonas and Stose (1938), but it is beyond the scope of this report to determine the type and relation of these structures.

Description of the Azimuthal Square-Array Direct-Current Resistivity Method

Direct-current, or d.c. resistivity methods have been used by a number of investigators to map bedrock fractures, but most of these studies have used colinear arrays, such as Wenner or Schlumberger arrays, that have been rotated about a common centerpoint to measure azimuthal variations in apparent resistivity that are related to fracture sets (Lewis and Haeni, 1987). The azimuthal square-array d.c. resistivity method has been successfully used to detect fracture strike in bedrock and it is more sensitive to anisotropy than the more commonly used Wenner or Schlumberger arrays (Lane and others, 1995). Another advantage of this method is that it requires about 65 percent less surface area than an equivalent survey using a Schlumberger or Wenner array (Lane and others, 1995). Habberjam (1979) presents a detailed discussion of the square-array method and techniques for data analysis. A recent paper by Lane and others (1995), which is cited throughout this report, is included in appendix A.

In the azimuthal technique, squares of increasing side length are expanded symmetrically about a common centerpoint, which is the location of the apparent resistivity measurements taken for each square. Measurements are taken in three directions (alpha, beta, and gamma) for each square (fig. 3). The alpha and beta measurements are taken perpendicular to each other and provide data on the directional variation of the apparent resistivity. The gamma measurement can be used to check the accuracy of the alpha and beta measurements (Lane and others, 1995). The concentric squares then are progressively rotated clockwise, typically at 15-degree intervals, about the common centerpoint so that directional variations in apparent resistivity with depth can be determined.

Acknowledgments

The authors thank the following people for their important contributions to this investigation. Thomas Meyer of the U.S. Army Corps of Engineers provided project support. John Lane and Eric White of the USGS Office of Ground Water, Branch of Geophysical Applications and Support are thanked for their assistance with field work and data compilation.

Methods

The following sections describe field methods for performing the square-array profiles and soundings, the electromagnetic terrain-conductivity survey, and methods used to analyze and interpret the data.

Field Methods

All data for the square-array profiles and soundings were collected using an ABEM Multimac d.c. resistivity system. This computer-controlled data acquisition and storage system allowed a complete sounding at a given azimuth to be collected automatically through remotely accessed addressable switchers, which connected electrodes for a given measurement (Lane and others, 1995). Electrode positions for the alpha, beta, and gamma directions of measurements are shown in figure 3. Software provided with the system was modified by Lane and others (1995) for the square array to control the measurement sequence.

Resistivity Profiles Two sets of parallel resistivity profiles were completed (fig. 1). The orientation of these profiles was 25°–205°. Profiles 1 and 2 were the westernmost of the two sets. Profile 1 extended to the main entrance road. Profile 2 was an extension of profile 1 that began on the southwest side of the main entrance road. Profile 3 was parallel to profile 1 and profile 4 was parallel to profile 2. The distance between the two sets of profiles was 25 m on center. Positions of the profiles were marked in the field with arrows painted on the road and fences so that points along the profiles could easily be located afterwards. These arrows pointed to the origin for profiles 1 and 3, to the points where these profiles crossed the road, and to the points on the other side of the road where profiles 1 and 3 continued as profiles 2 and 4, respectively.
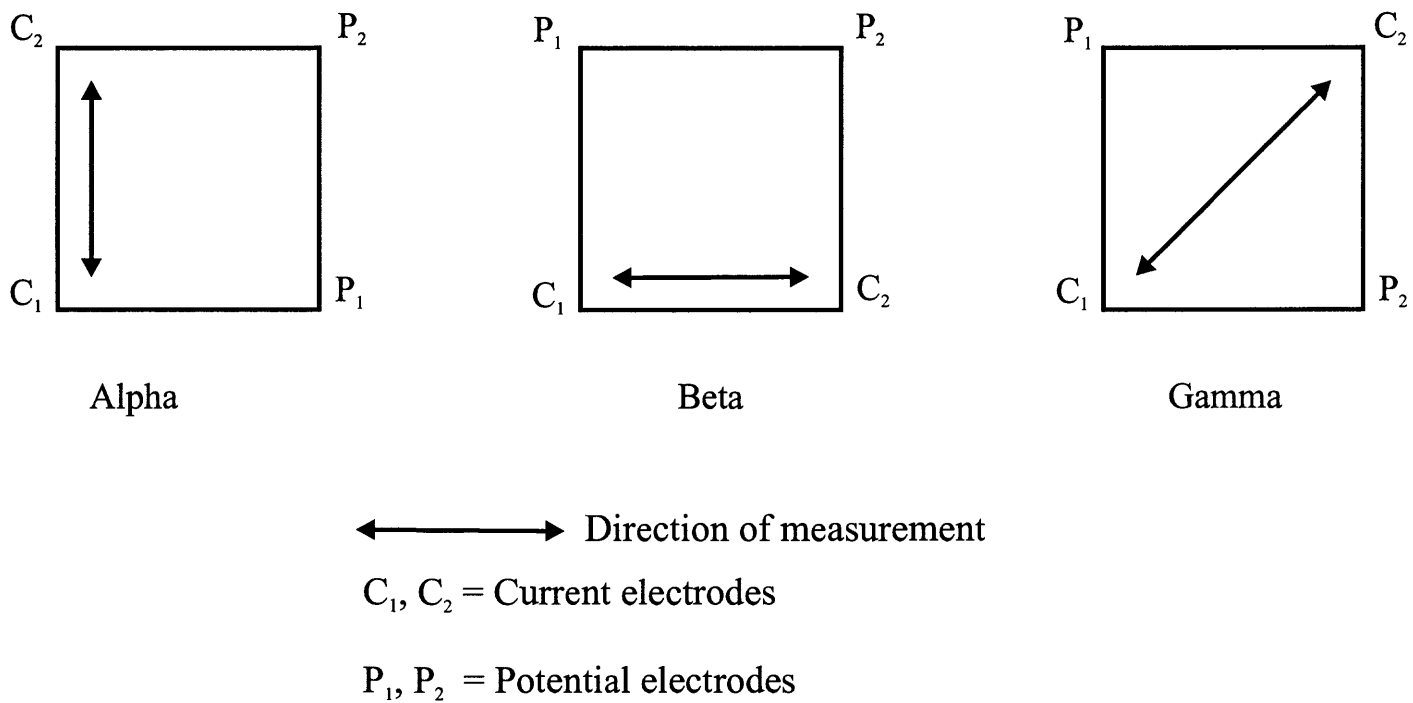
Figure 3 . Electrode configurations for square-array direct-current resistivity measurements (modified from Lane and others, 1995).

Each profile consisted of overlapping squares that were 10 m in length along a side (fig. 4). Adjacent squares overlapped by 5 m to provide some data redundancy. In addition to a series of squares that were oriented 25°–205° (referred to herein as "non-rotated squares"), another series of squares (referred to as "rotated squares") were oriented 45° to the 25°–205° trend (2 parallel sides of the rotated square trended 70°–250° and the other 2 parallel sides trended 160°–340°) (fig. 4).

Resistivity Soundings Three resistivity soundings were performed after the profiles were completed and the data were reviewed. Soundings 1 and 2 were conducted between profiles 1 and 3 (fig. 1). The centerpoint for sounding 1 was located at the midpoint between profiles 1 and 3, along the origin line. Sounding 2 also was located at a midpoint between profiles 1 and 3 that was 60 m southwest of the centerpoint for sounding 1. Sounding 3 was in a field approximately 760 m southwest of the location of sounding 1 (fig. 1). This site was selected to collect background information on the Frederick Limestone at some distance away from the suspected structure. Each sounding consisted of a set of 6 concentric squares with the following side lengths: 4.24, 7.07, 9.90, 14.14, 19.80, and 28.28 m. These squares initially were oriented at 350°, along the line between the potential electrodes in the alpha electrode configuration (fig. 3). After the initial set of readings was completed, the squares progressively were rotated clockwise about the array centerpoint in 15-degree increments to azimuths of 5°, 20°, 35°, 50°, and 65°. A complete set of readings was taken at each orientation; alpha measurements were made between 350° and 65° and beta measurements were made between 80° and 155°.

Electromagnetic Terrain-Conductivity Survey A Geonics EM-34 electromagnetic terrain-conductivity meter was used to determine if the PVC gas pipeline buried along the shoulder of the road would have any effect on the square-array resistivity readings. A short survey approximately 32 m long was performed. This survey began in the field where profiles 1 and 3 were completed, crossed the road, and ended in the field on the west side of the road (fig. 1).

Analytical Methods

The resistivity profiles and soundings 1 and 2 were interpreted on the basis of methods described in Lane and others (1995), which are based largely on a method described by Habberjam (1972). Field data were entered into a spreadsheet and apparent resistivity was calculated on the basis of a geometric factor for the array, the voltage potential difference (measured between electrodes P1 and P2; fig. 3), and the current (measured between electrodes C1 and C2; fig. 3). For the purposes of this report, an anomaly was considered to be a point or cluster of points that was clearly outside the trend of nearby points, and was determined on the basis of observation rather than defined by quantitative criteria.

Non-rotated squares

Square 1

MP 1

10 meters

MP 2

Square 2

Profile

5 meters

Measuring points (MP)

Rotated squares

Square 1

10 meters
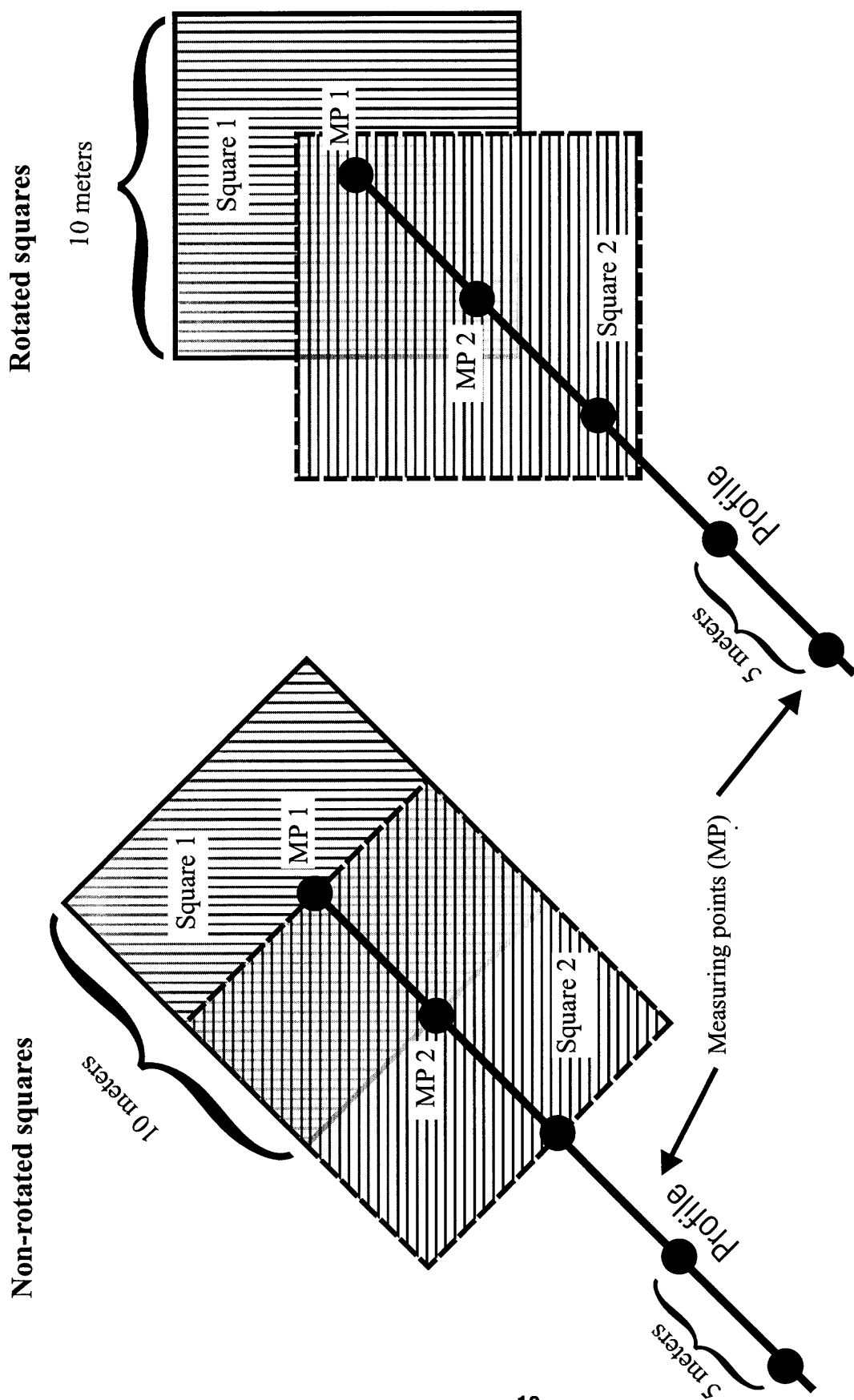
MP 1

MP 2

Square 2

Profile

5 meters

Figure 4. Square-array layouts used along profiles 1-4. Non-rotated squares are shown on the left and rotated squares are shown on the right.

10

For all squares in soundings 1-3, the fracture strike was determined graphically by plotting the apparent resistivity for each of the square arrays against the azimuth of that measurement. The principal fracture strike is interpreted to be perpendicular to the direction of maximum resistivity (Lane and others, 1995). In cases in which there were some high values of apparent resistivity for a given square, trends in nearby data points also were considered. That is, the highest apparent resistivity value was not selected if it was an obvious spike rather than an identifiable trend in the data from adjacent points. The few data points that were erroneous due to poor electrical connections have been removed from the plots and data table. Because sounding 3 showed little anisotropy, it was difficult to use this graphical technique to determine the fracture strike direction. The program FITELLIPSE by Hart and Rudman (1997) also was used. This program calculates the orientation and values of the major and minor axes of a best-fit ellipse to the data. This program was used on all squares in sounding 3 and also was used to compare the graphical solutions in all squares in soundings 1 and 2.

Results of Resistivity Profiles, Resistivity Soundings, and Terrain-Conductivity Survey

Results of the resistivity profiles, resistivity soundings, and the terrain-conductivity survey are presented in the following sections.

Resistivity Profiles

The mean geometric resistivity along profiles 1-4 is shown in figure 5. Apparent anisotropy for profiles 1-4 is shown in figure 6. For profiles 1 and 2, the apparent resistivity for non-rotated squares is shown in figure 7 and for rotated squares is shown in figure 8. For profiles 3 and 4, the apparent resistivity for non-rotated squares is shown in figure 9 and for rotated squares is shown in figure 10. A plot of the anomalies along profiles 1 and 3 is presented in figure 11.

Profiles 1 and 2 Although there are strong upward spikes in the interval between 40 and 55 m and an increasing trend near the road, the mean geometric resistivity generally decreases from northeast to southwest along profiles 1 and 2 (fig. 5). Pronounced changes in apparent anisotropy along profiles 1 and 2 occur between 35 to 65 m and between 75 to 100 m (fig. 6). The alpha, beta, and gamma readings for profiles 1 and 2 for the non-rotated squares are shown in figure 7. In the alpha configuration, there were changes in apparent resistivity in the interval between 40 and 55 m, particularly between 40 and 45 m, where the apparent resistivity increased by 31 ohm-meters. The gamma reading also showed changes (indicating anisotropy) in the interval between 35 and 65 m, particularly between 55 and 60 m and between 60 m and 65 m (fig. 7). Between 90 and 95 m, the beta reading dropped 28 ohm-meters, and the gamma showed 43 ohm-meters of difference between the alpha and beta readings (fig. 7). On the rotated squares (fig. 8), the alpha readings showed changes at 25 m, in the interval between 35 and 55 m, at 80 m, and at 95 m; the beta readings showed changes between 50 and 55 m and at 95 m; and pronounced differences were observed in the gamma readings between 50 to 55 m, at 85 m, and at 95 m.
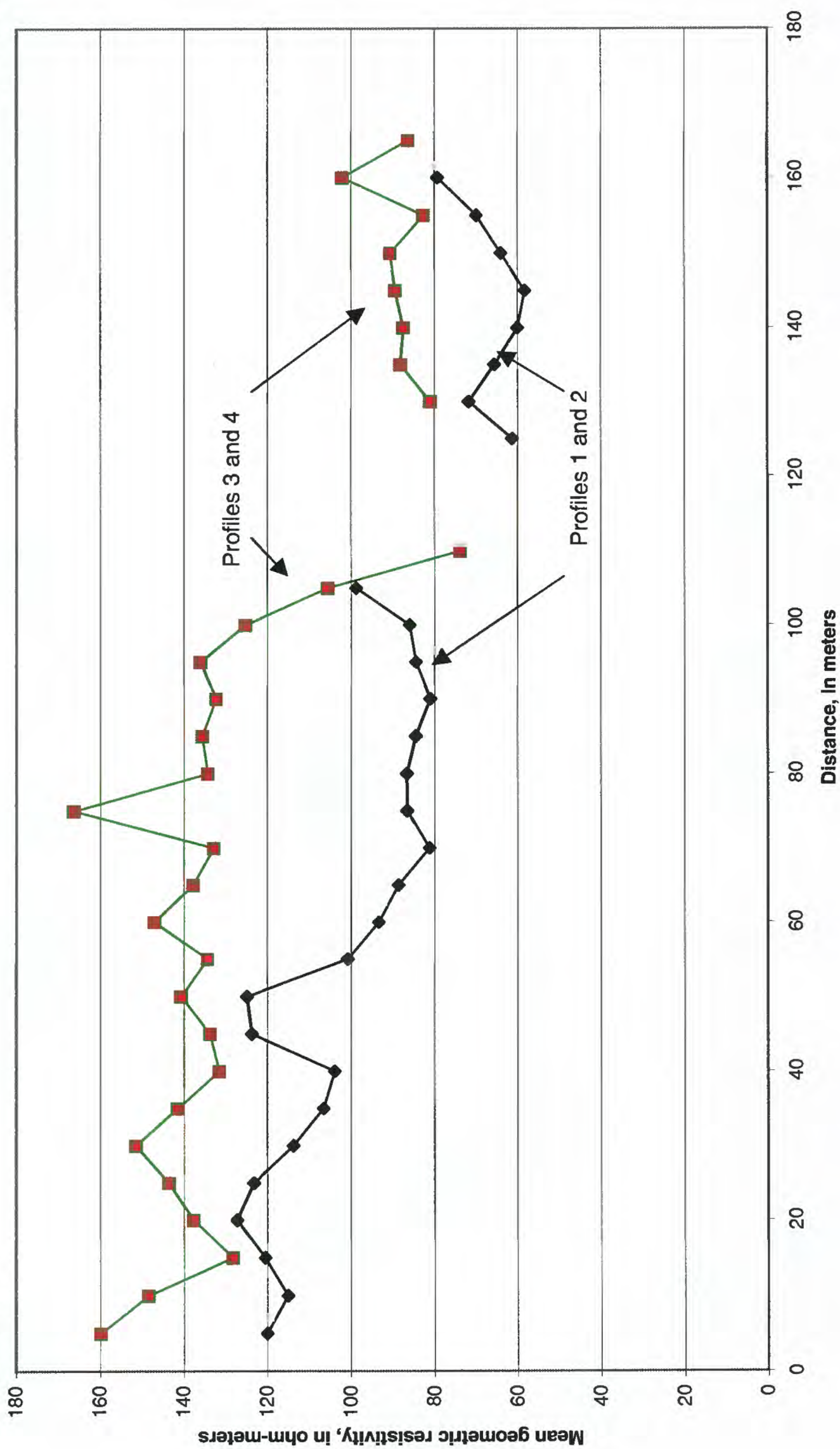
Figure 5. Mean geometric resistivity plotted against distance along profiles 1 - 4, Fort Detrick, Maryland.
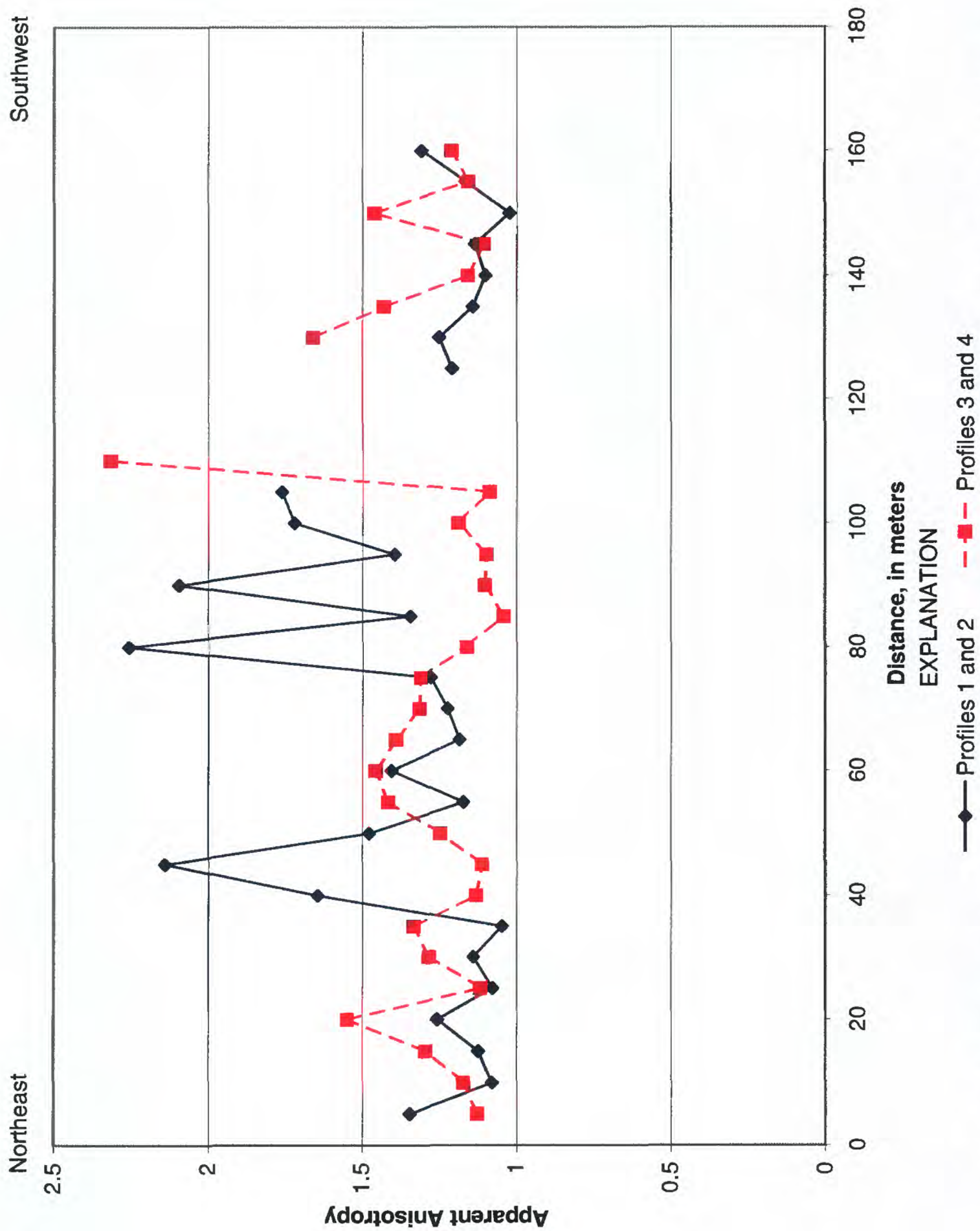
Figure 6. Apparent anisotropy plotted against distance along profiles 1 - 4, Fort Detrick, Maryland.

13

Figure 7. Apparent resistivity of non-rotated squares plotted against distance along profiles 1 and 2, Fort Detrick, Maryland.

14

Figure 8. Apparent resistivity of rotated squares plotted against distance along profiles 1 and 2, Fort Detrick, Maryland

Figure 9. Apparent resistivity of non-rotated squares plotted against distance along profiles 3 and 4, Fort Detrick, Maryland.
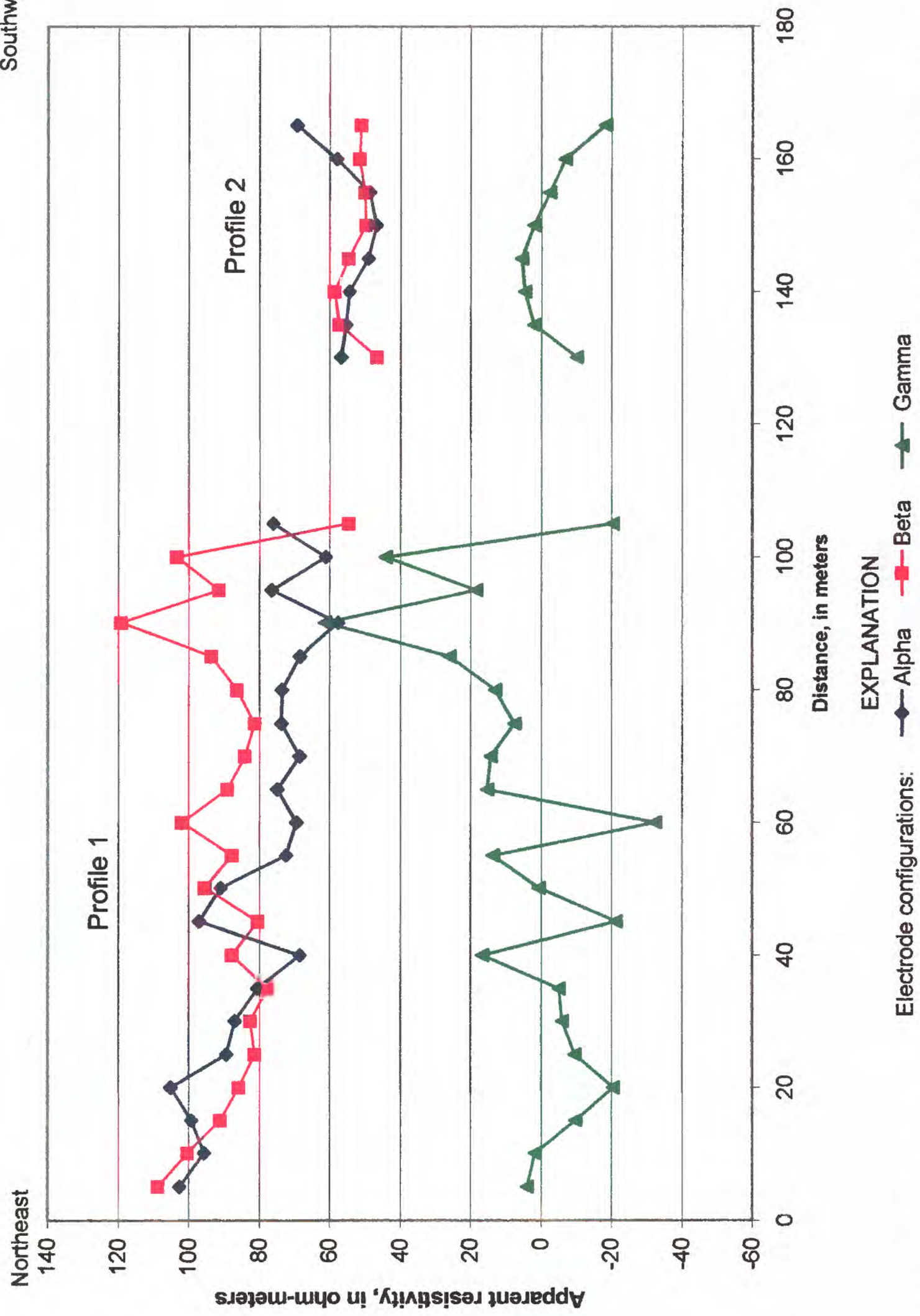
16

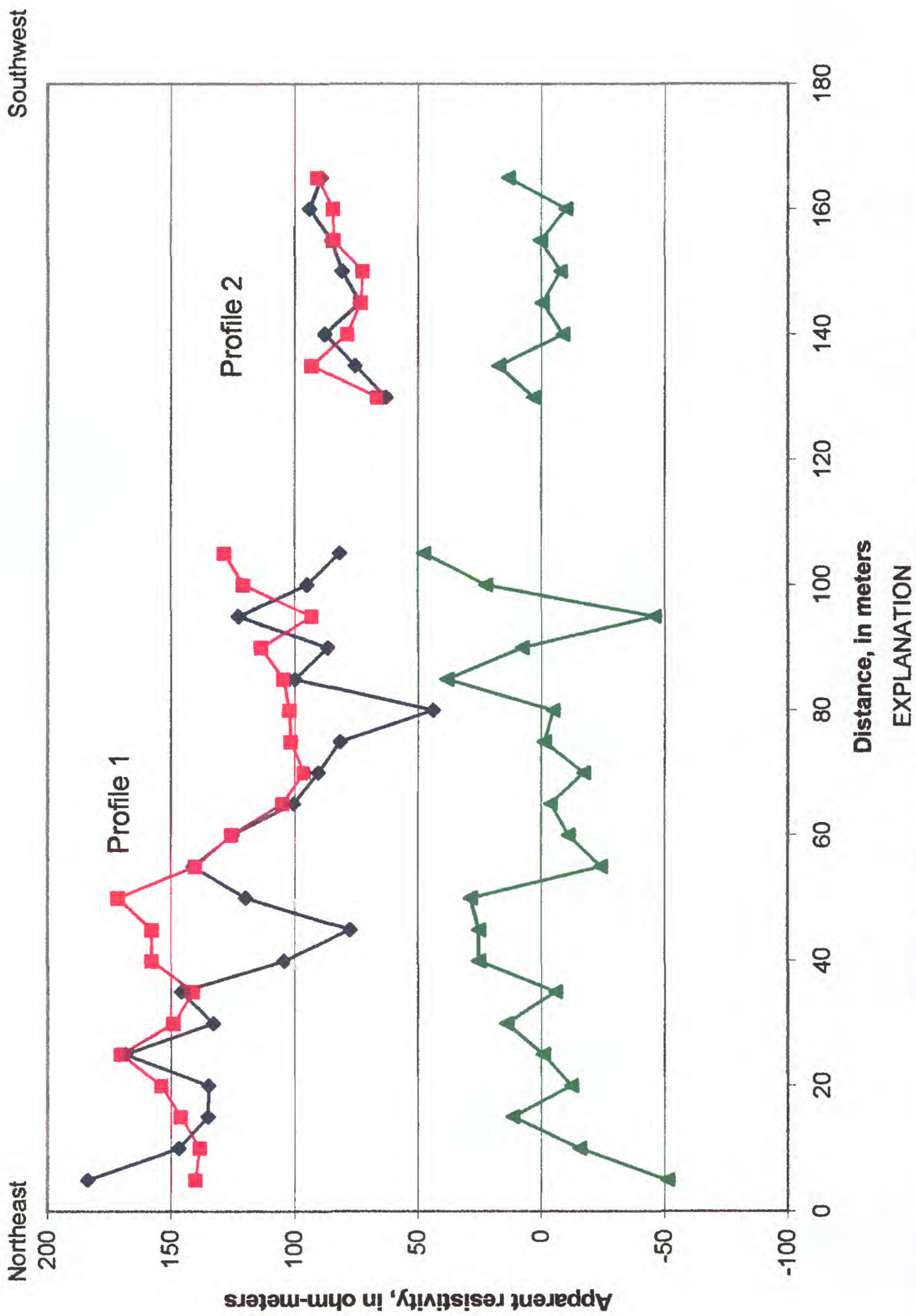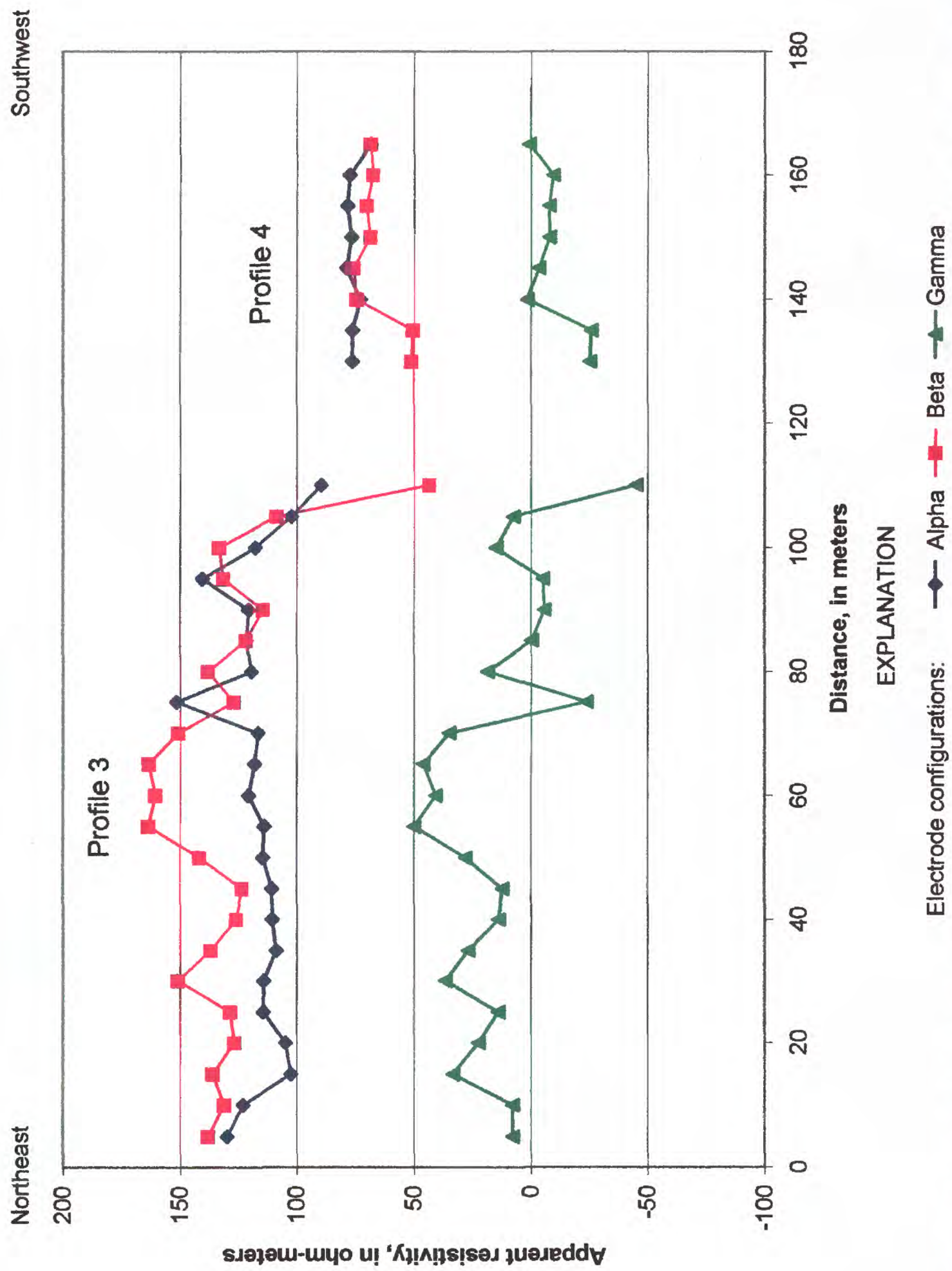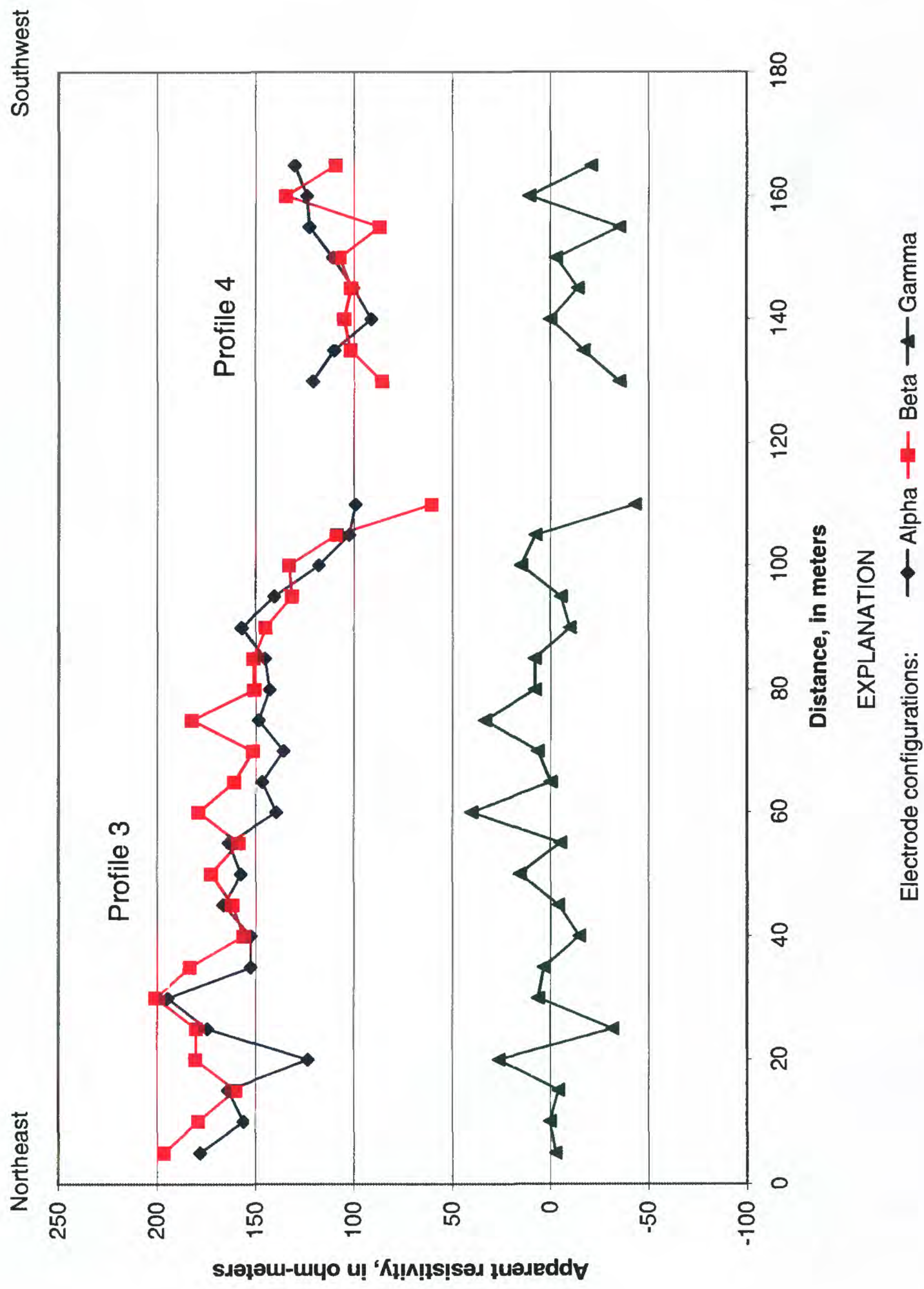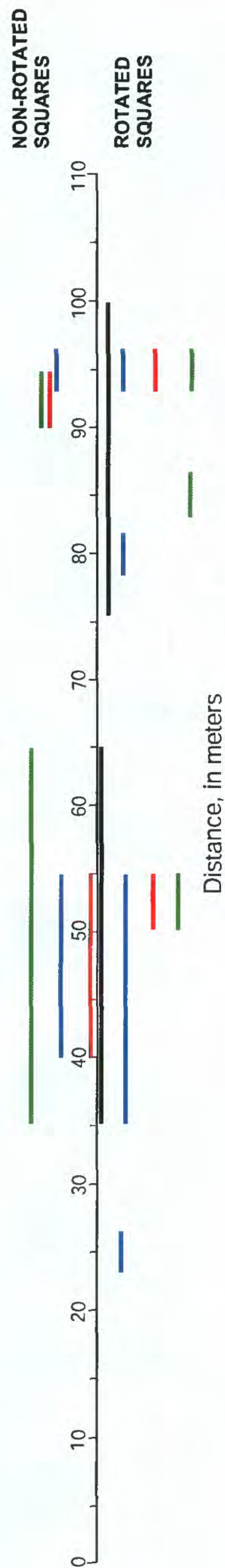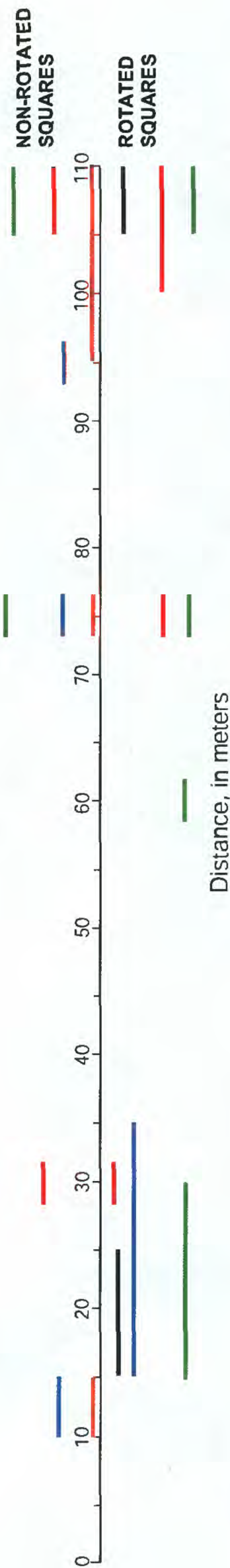Figure 10. Apparent resistivity of rotated squares plotted against distance along profiles 3 and 4, Fort Detrick, Maryland.

Figure 11. Apparent resistivity anomalies along profiles 1 and 3, Fort Detrick, Maryland

In summary, the mean geometric resistivity showed an overall decrease along profiles 1 and 2. Anomalies in apparent resistivity were observed in the non-rotated squares in the intervals between 35 to 65 m, between 90 to 95 m, and at 95 m. In the rotated squares, anomalies were observed at 25 m, in the interval between 35 to 55 m, and at 80 m, 85 m, and 95 m.

Profiles 3 and 4 As in profiles 1 and 2, the mean geometric resistivity generally decreased from northeast to southwest along profiles 3 and 4 (fig. 5). The most pronounced change was a drop of 62 ohm-meters in the interval between 95 to 110 m. Smaller changes were observed between 10 and 15 m and at 75 m. The most pronounced changes in apparent anisotropy along profiles 3 and 4 were observed between 15 to 25 m and between 105 to 110 m (fig. 6). The alpha, beta, and gamma readings for profiles 3 and 4 for the non-rotated squares are shown in figure 9. Alpha anomalies were observed between 10 and 15 m, and at 75 m and 95 m. Beta anomalies were observed at 30 m and between 105 to 110 m. Gamma anomalies were observed at 75 m and between 105 to 110 m. Alpha, beta, and gamma values all decreased fairly sharply in the interval between 100 to 110 m. On the profiles for the rotated squares (fig. 10), there was an anomaly in the alpha reading between 15 to 35 m, anomalies in the beta readings at 75 and between 100 to 110 m, and in the gamma readings from 15 to 30 m, at 60 m and at 75 m, and between 105 to 110 m.

In summary, the mean geometric resistivity generally decreased from northeast to southwest along profiles 3 and 4, with the largest decline between 95 to 110 m. Anomalies in apparent resistivity were observed in the non-rotated squares in the interval between 10 to 15 m, at 30 m, at 75 m, at 95 m, and from 105 to 110 m. In the rotated squares, anomalies were observed at 15 to 35 m, at 60 m, at 75 m, and from 95 to 110 m.

Resistivity Soundings

Data for the soundings are presented in table 1 and are plotted as apparent resistivity with respect to azimuth in figures 12-20. Fracture strike directions for soundings 1-3 determined by use of graphical methods and the FITELLIPSE approach (Hart and Rudman, 1997) are shown in table 2.

The maximum depth of penetration of a given sounding would be equivalent to the length of the side of the square (the A-spacing), but the depth of penetration is usually less and is affected by the resistivities of the various layers, which are affected by porosity, water content, water quality, and the rock matrix (John Lane, U.S. Geological Survey, oral commun., 1998).

Sounding 1 Plots of apparent resistivity and azimuth are shown for squares 1-3 in figure 12, for squares 4-6 in figure 13, and for squares 1-6 in figure 14. In squares 1 and 2, the primary fracture strike based on the graphical method was 110° and 95°, respectively, and the interpreted highest apparent resistivity decreased with depth from 263 to 204 ohm-meters (fig. 12). In square 3, the primary fracture strike based on the graphical method was 50°. In squares 4-6, the primary fracture strike was 65°, 65°, and 50°, respectively, and the interpreted highest apparent resistivity increased with depth from 250 ohm-meters in square 4 to 423 ohm-meters in square 5, but decreased to 300 ohm-meters in square 6 (fig. 13; table 1). The shapes of the plots are appreciably different between squares 1-3 and 4-6, but both show strong directional trends.

Table 1. Azimuthal apparent resistivity for soundings 1-3, Area B, Fort Detrick, Maryland

[Location of soundings are shown in figure 1; m, meters; --, data points missing because of poor electrical connections]

Sounding 1

A-spacing (m)	Geometric Factor	Mean	Azimuth, in degrees from true north — Apparent resistivity, in ohm-meters											
			350	5	20	35	50	65	80	95	110	125	140	155
4.24	45.51	208.8	251.7	259.8	262.6	225.3	180.7	251.7	170.7	172.5	171.1	186.6	217.5	156.1
7.07	75.84	180.5	203.3	204.0	203.3	169.1	150.9	216.9	157.0	169.9	175.2	188.9	198.0	129.7
9.90	106.18	175.1	182.6	160.3	171.0	157.2	152.9	203.9	172.0	178.4	191.1	190.1	194.3	147.6
14.14	151.69	193.4	200.2	185.1	169.9	166.9	172.9	183.5	191.1	185.1	207.8	204.8	203.3	250.3
19.80	212.37	231.7	278.2	210.2	212.4	169.9	182.6	216.6	208.1	201.7	214.5	225.1	237.8	422.6
28.28	303.38	249.8	273.0	285.2	282.1	248.8	--	260.9	257.9	248.8	270.0	285.2	300.3	236.6

Sounding 2

A-spacing (m)	Geometric Factor	Mean	Azimuth, in degrees from true north — Apparent resistivity, in ohm-meters											
			350	5	20	35	50	65	80	95	110	125	140	155
4.24	45.51	83.1	90.6	80.1	--	87.8	92.4	81.9	89.2	96.0	98.7	92.4	89.6	98.7
7.07	75.84	111.6	110.0	111.5	111.5	112.3	106.9	103.1	111.5	110.0	111.5	112.3	118.3	120.6
9.90	106.18	135.3	132.7	140.2	140.2	140.2	129.5	125.3	128.5	128.5	133.8	133.8	144.4	146.5
14.14	151.69	163.8	177.5	120.0	171.4	166.9	154.7	150.2	147.1	154.7	162.3	179.0	182.0	200.2
19.80	212.37	209.2	237.8	223.0	206.0	191.1	180.5	167.8	163.5	189.0	212.4	231.5	248.5	259.1
28.28	303.38	267.2	291.2	303.4	282.1	260.9	233.6	227.5	224.5	242.7	257.9	273.0	300.3	309.4

Sounding 3

A-spacing (m)	Geometric Factor	Mean	Azimuth, in degrees from true north — Apparent resistivity, in ohm-meters											
			350	5	20	35	50	65	80	95	110	125	140	155
4.24	45.51	518.0	--	446.9	480.6	572.0	505.1	502.9	450.5	498.8	427.3	371.8	410.5	496.0
7.07	75.84	320.2	275.3	291.2	321.6	377.7	358.7	289.0	354.2	293.5	289.0	298.8	302.6	390.6
9.90	106.18	278.9	225.1	231.5	243.2	292.0	321.7	250.6	319.6	268.6	275.0	289.9	282.4	347.2
14.14	151.69	252.7	219.9	--	227.5	276.1	309.4	229.1	277.6	285.2	303.4	277.6	250.3	301.9
19.80	212.37	277.0	265.5	263.3	250.6	299.4	259.1	259.1	278.2	303.7	344.0	254.8	276.1	269.7
28.28	303.38	381.0	312.5	--	321.6	270.0	263.9	336.8	348.9	358.0	452.0	439.9	418.7	312.5

Table 2. Fracture-strike directions for soundings 1-3 determined by use of graphical methods and program FITELLIPSE[1], Fort Detrick, Maryland

[m, meters; °, degrees; azimuth directions are shown in degrees from true north]

Square number	Square size (m)	Sounding 1		Sounding 2		Sounding 3	
		Graphical	FITELLIPSE	Graphical	FITELLIPSE	Graphical	FITELLIPSE
1	4.24	110°	107°	65°	29°	125°	130°
2	7.07	95°	97°	65°	58°	125°	114°
3	9.90	50°	19°	65°	76°	140°	19°
4	14.14	65°	50°	65°	64°	140°	6°
5	19.80	65°	62°	65°	63°	20°	12°
6	28.28	50°	62°	65°	73°	20°	29°

[1]Hart and Rudman, 1997
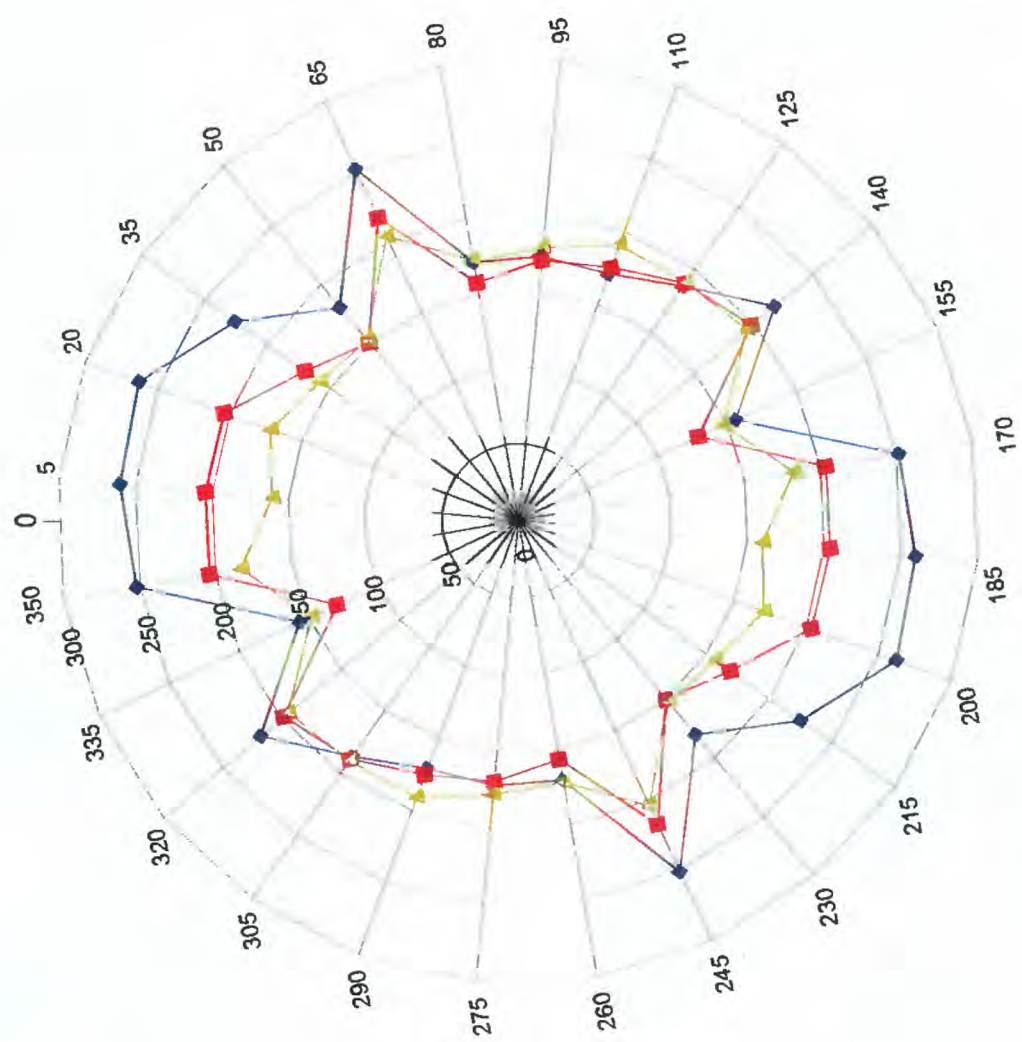
Figure 12. Azimuth and resistivity, in ohm-meters, for sounding 1, squares 1-3, Fort Detrick, Maryland.

EXPLANATION

Square-array side length, in meters (A-spacing)

4.24   7.07   9.90

EXPLANATION

Square-array side length, in meters (A-spacing)

— 14.14   — 19.80   — 28.28

Figure 13. Azimuth and resistivity, in ohm-meters, for sounding 1, squares 4-6, Fort Detrick, Maryland.

Figure 14. Azimuth and resistivity, in ohm-meters, for sounding 1, squares 1-6, Fort Detrick, Maryland.

EXPLANATION

Square-array side length, in meters (A-spacing)

4.24   7.07   9.90   14.14   19.80   28.28

Figure 15. Azimuth and resistivity, in ohm-meters, for sounding 2, squares 1-3, Fort Detrick, Maryland.

Figure 16. Azimuth and resistivity, in ohm-meters, for sounding 2, squares 4-6, Fort Detrick, Maryland.

Figure 17. Azimuth and resistivity, in ohm-meters, for sounding 2, squares 1-6, Fort Detrick, Maryland.
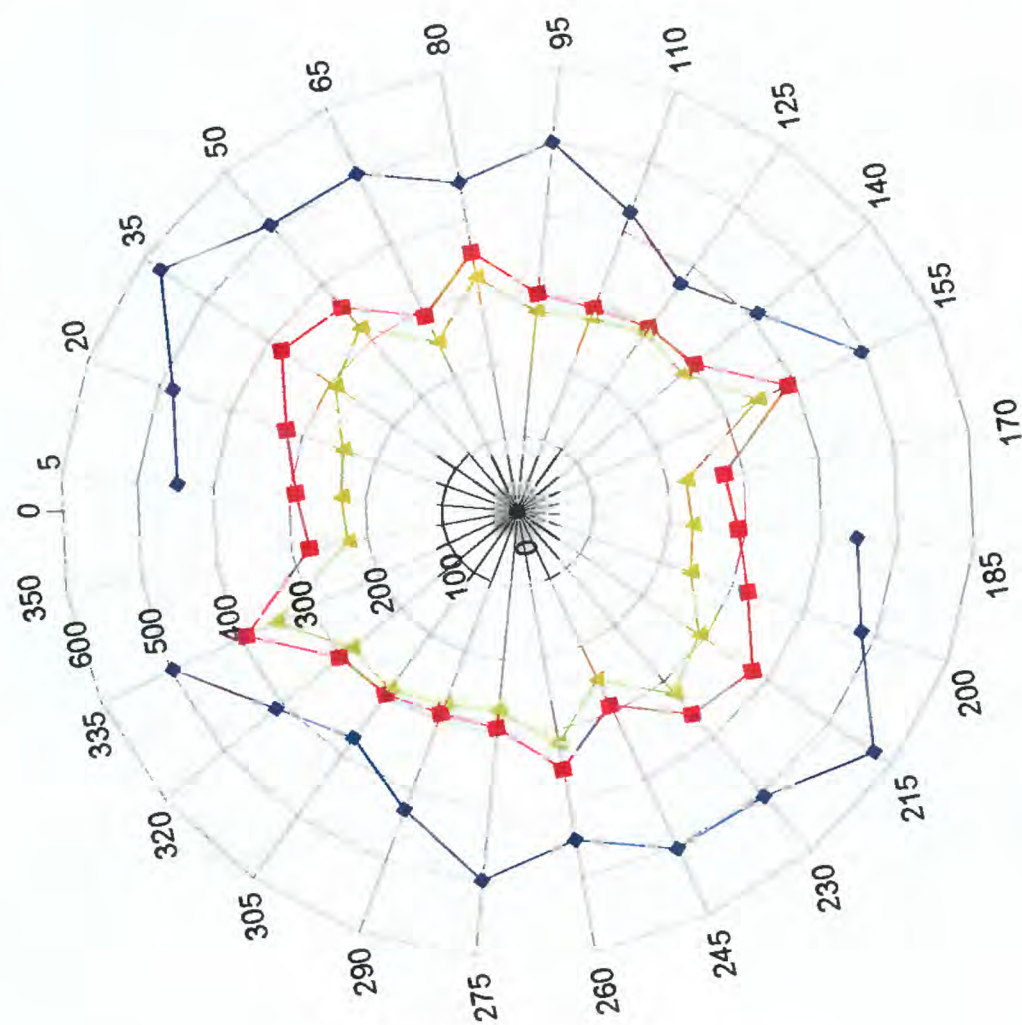
Figure 18. Azimuth and resistivity, in ohm-meters, for sounding 3, squares 1-3, Fort Detrick, Maryland.

EXPLANATION

Square-array side length, in meters (A-spacing)
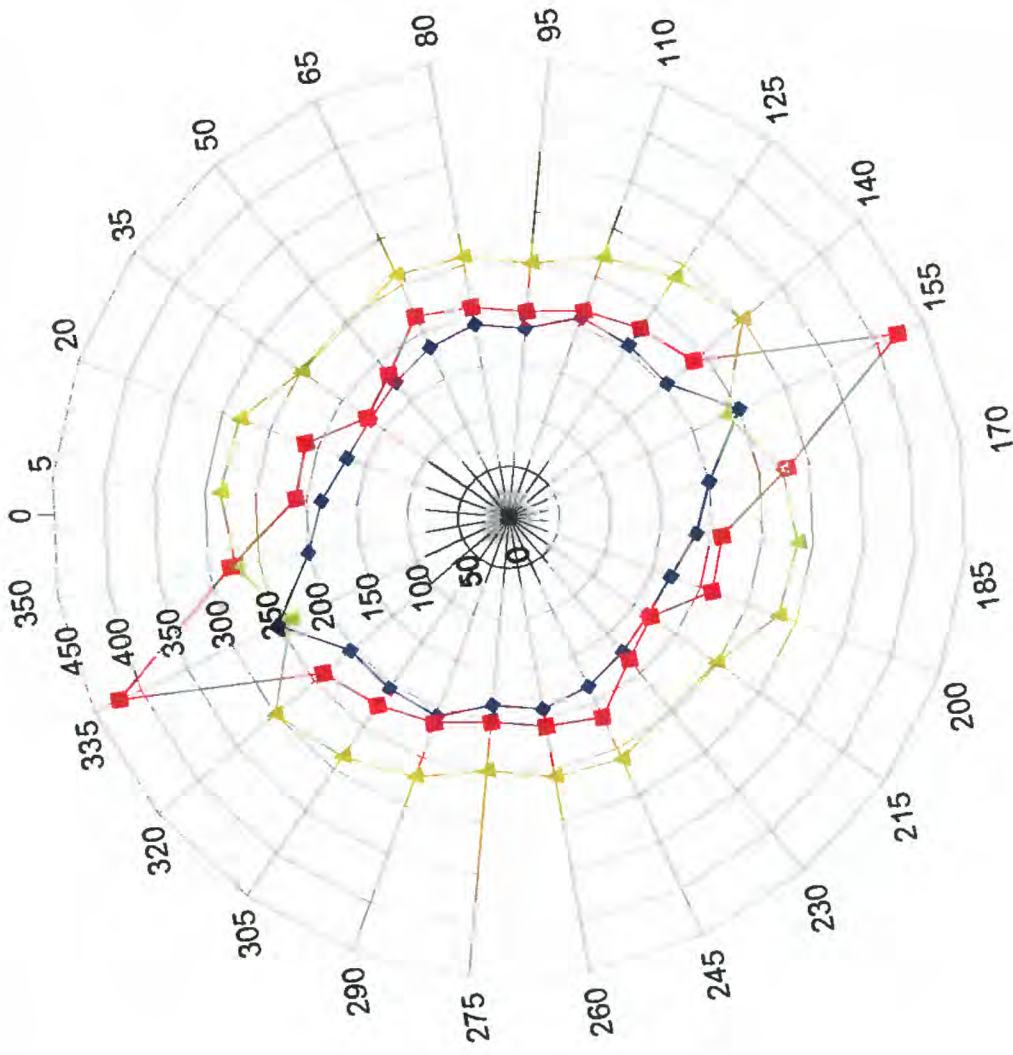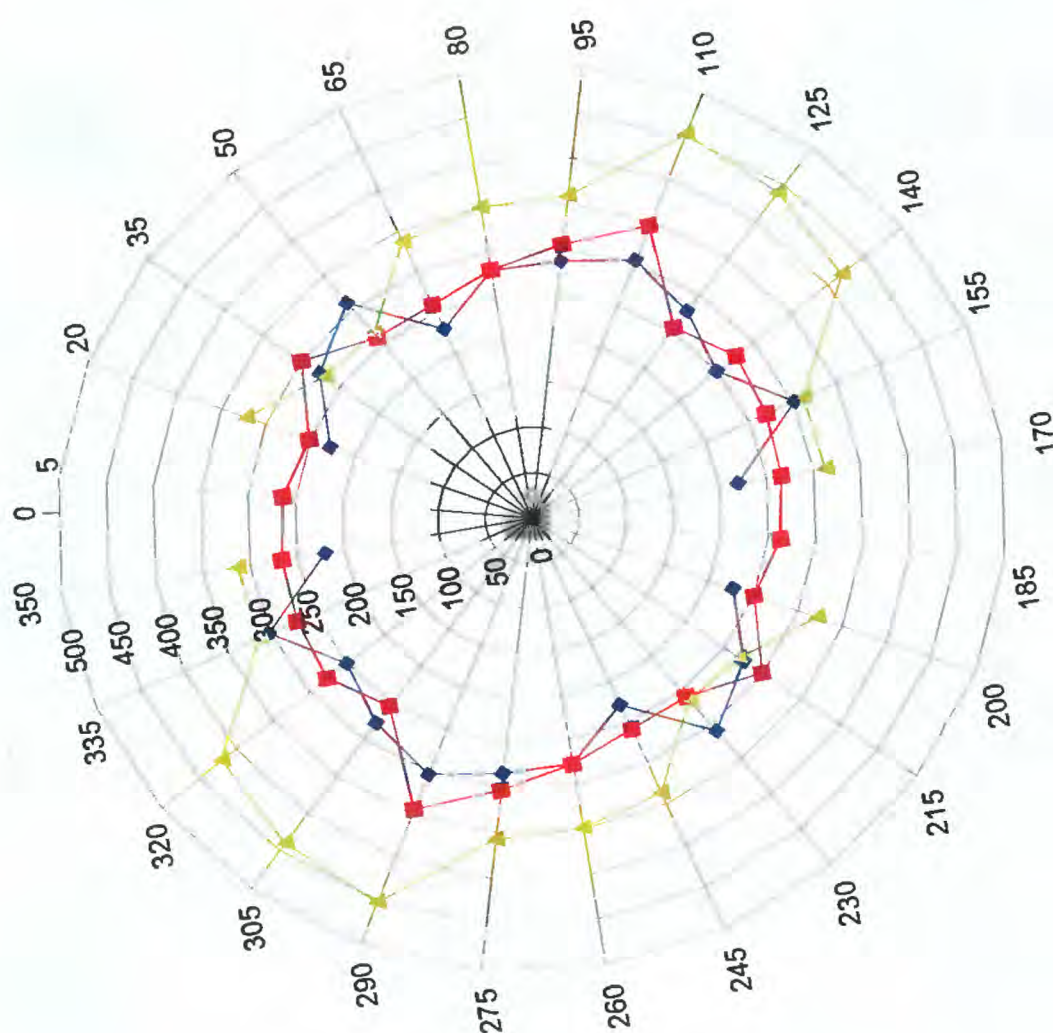
◆ 4.24   ■ 7.07   ▲ 9.90

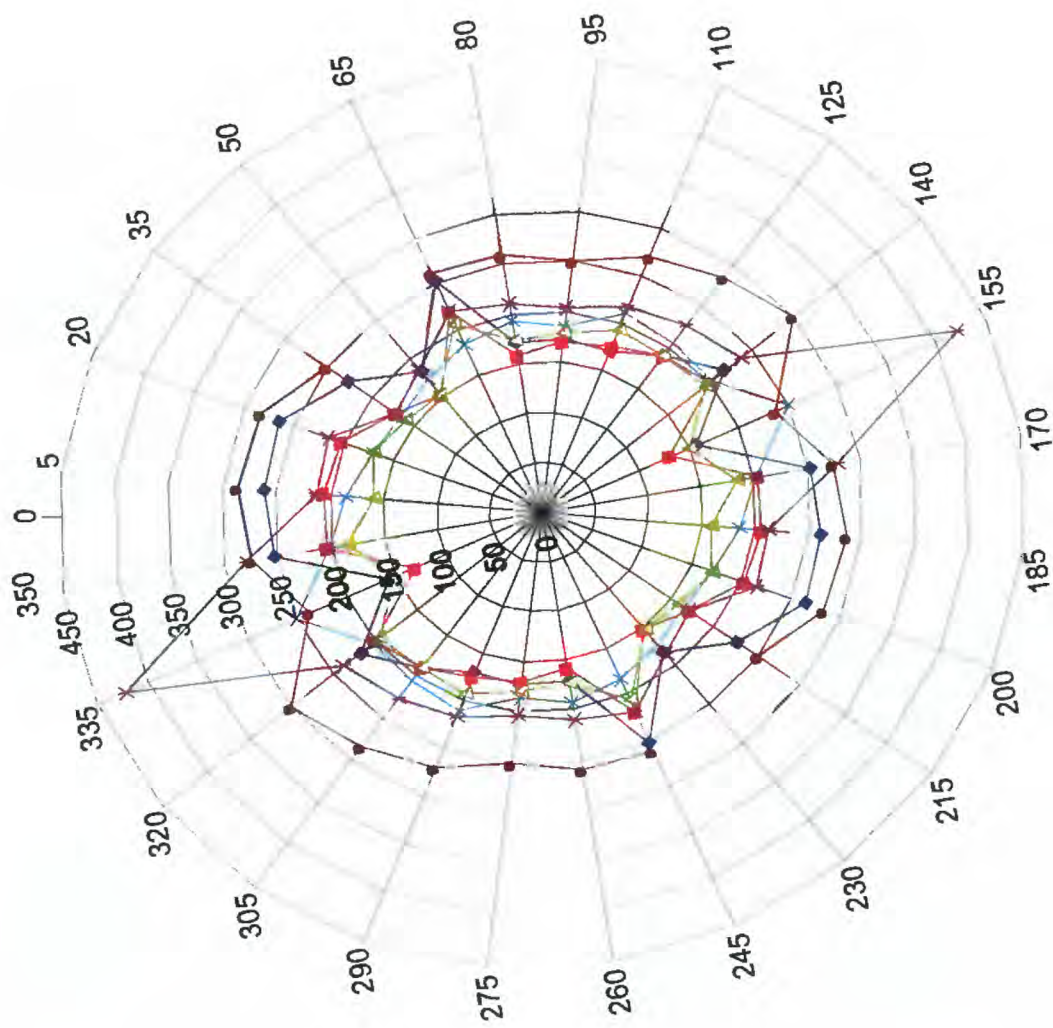EXPLANATION

Square-array side length, in meters (A-spacing)

14.14   19.80   28.28

Figure 19. Azimuth and resistivity, in ohm-meters, for sounding 3, squares 4-6, Fort Detrick, Maryland.
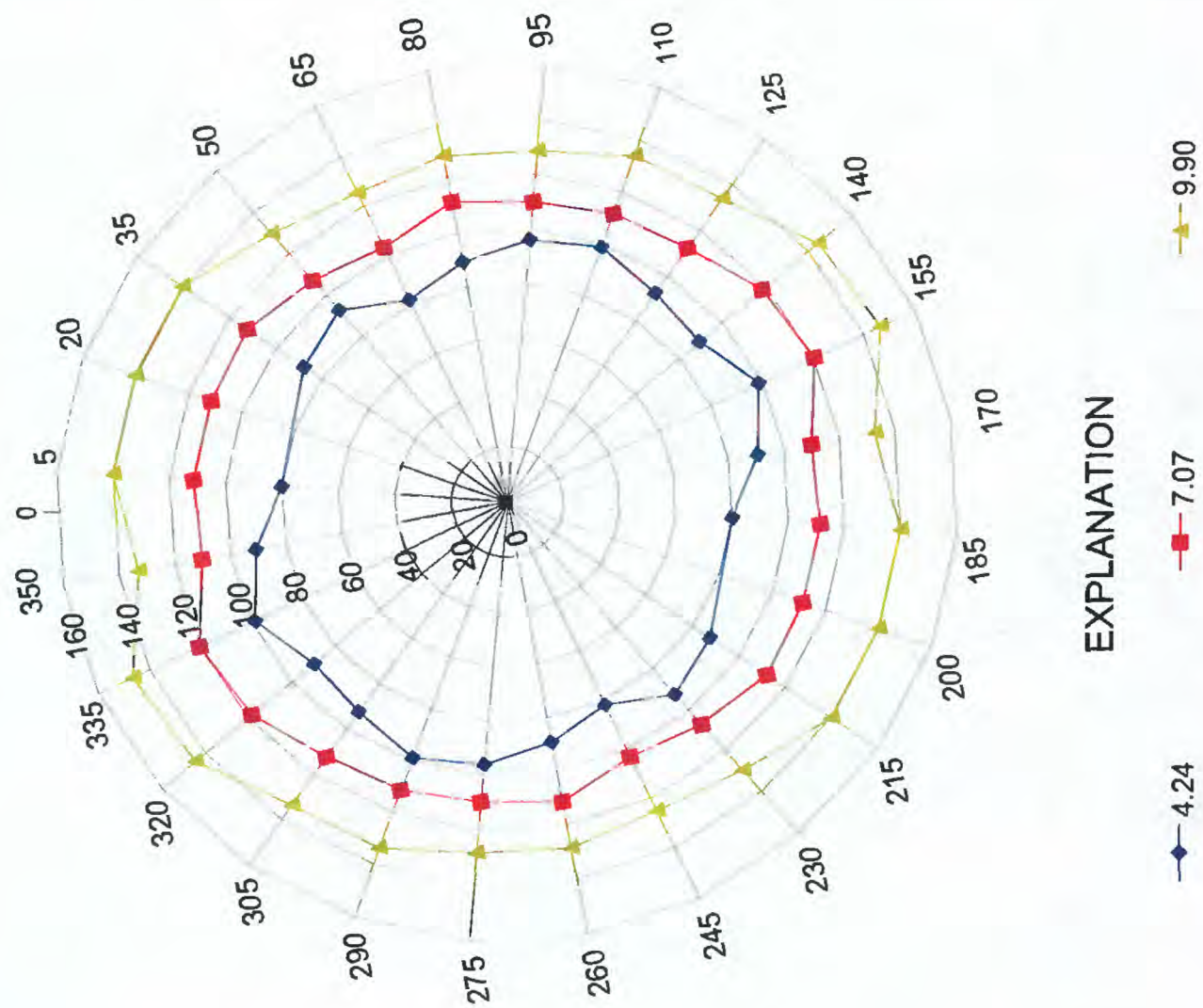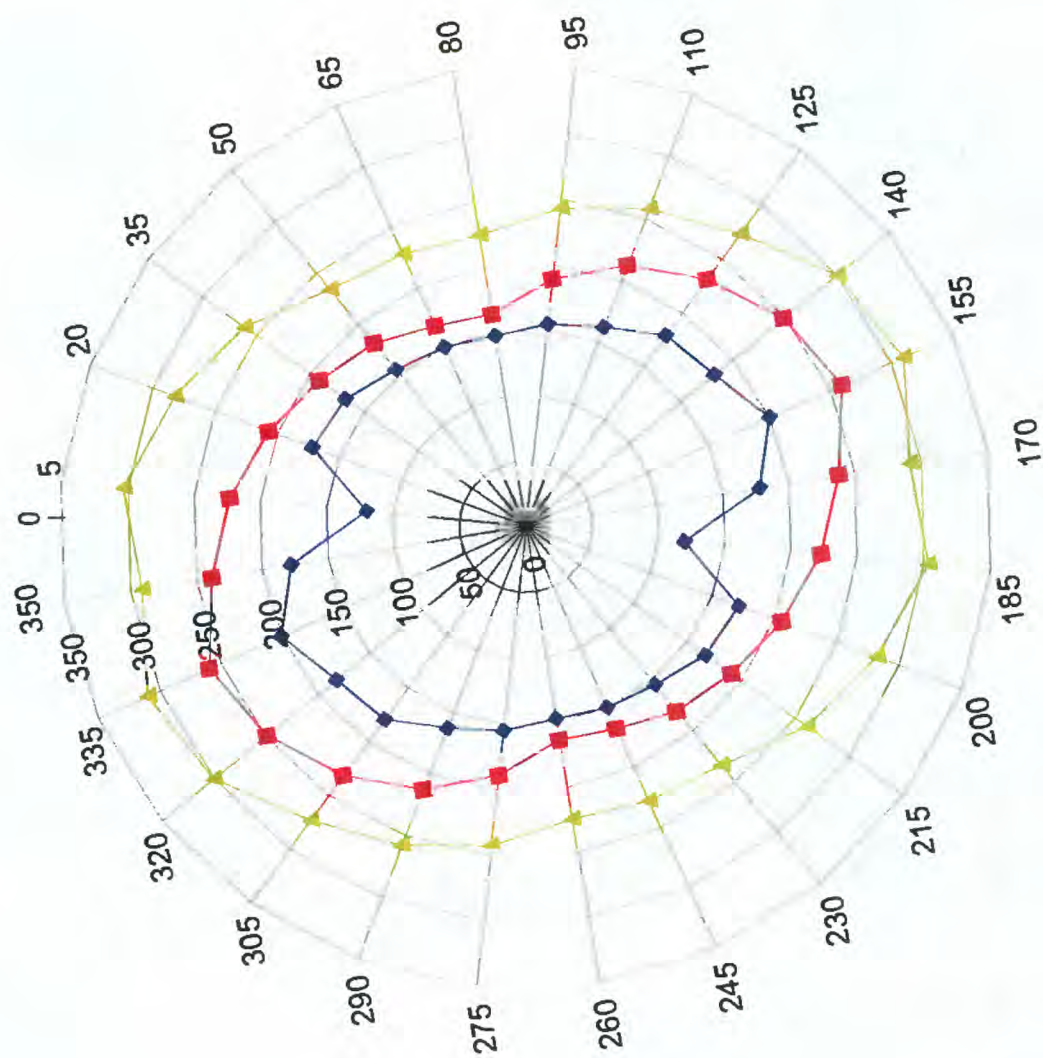
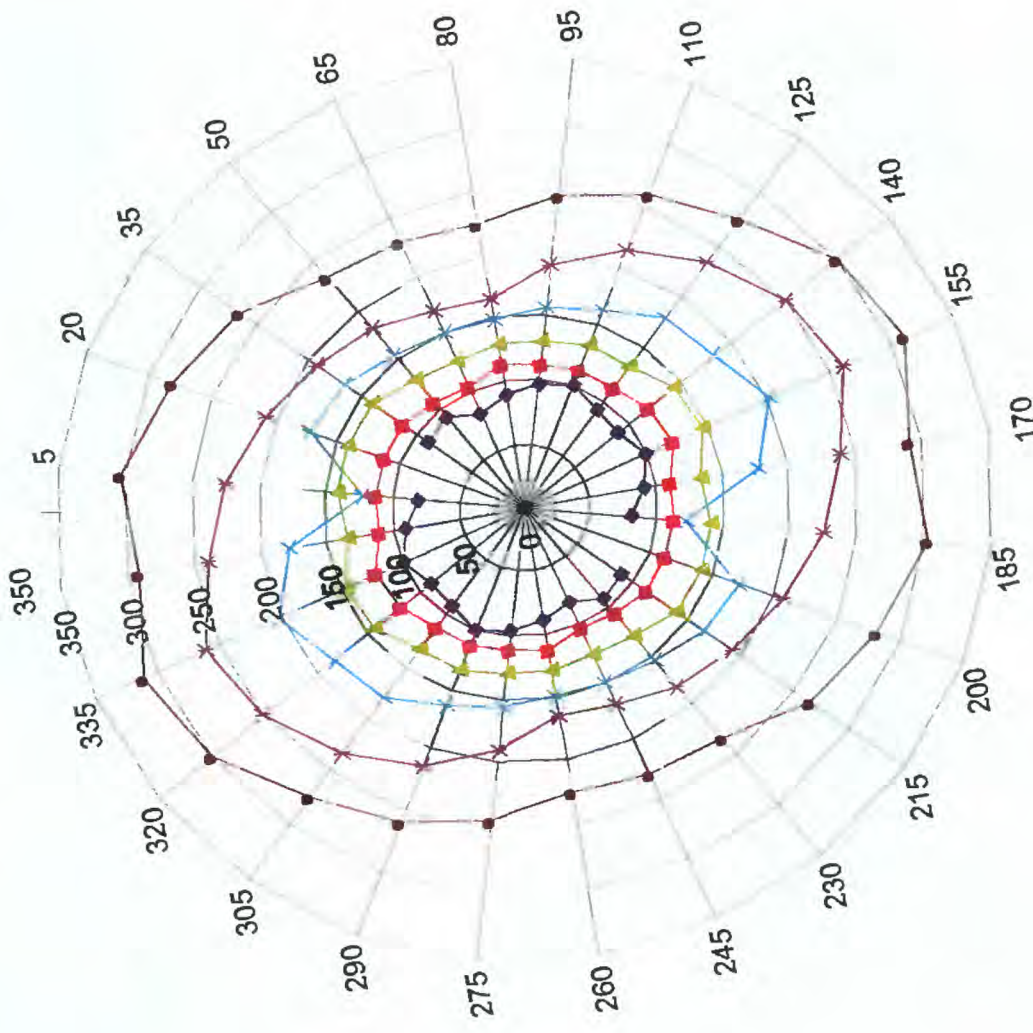**Figure 20.** Azimuth and resistivity, in ohm-meters, for sounding 3, squares 1-6, Fort Detrick, Maryland.

EXPLANATION

Square-array side length, in meters (A-spacing)

4.24 ■ 7.07 9.90 14.14 19.80 28.28
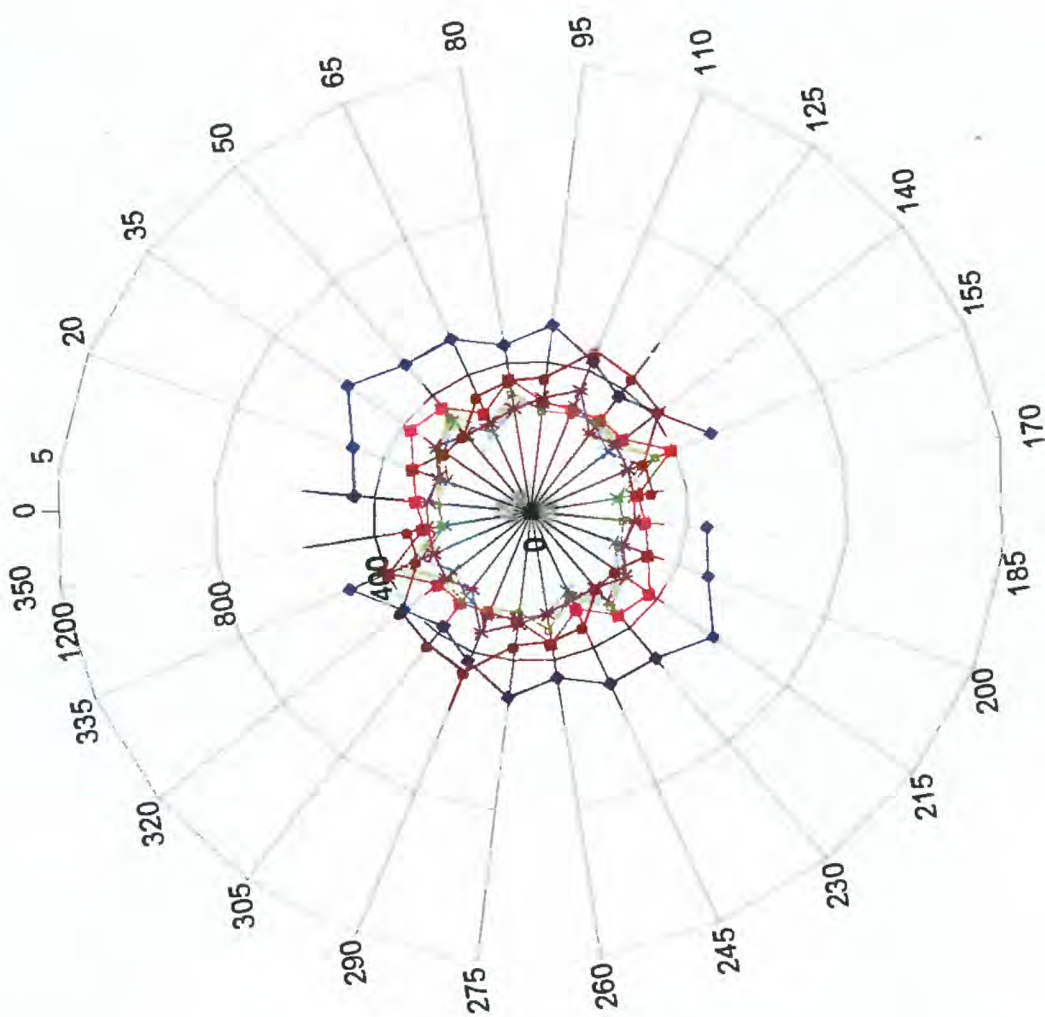
Sounding 2 Plots of apparent resistivity and azimuth are shown for squares 1-3 in figure 15, for squares 4-6 in figure 16, and for squares 1-6 in figure 17. The highest interpreted apparent resistivity values increased with depth from a minimum of 80 in square 1 to a maximum of 309 ohm-meters in square 6 (table 2). In squares 1-3, the primary fracture strike based on the graphical method was somewhat poorly defined but probably was about 65°. In squares 4-6, the primary fracture strike determined graphically was better defined and also was 65°. The plot shapes are somewhat similar, but the trends are better defined in the plots of squares 4-6, which are more elliptical and, therefore, more anisotropic, indicating stronger trends in the fracture orientation.

Sounding 3 Plots of apparent resistivity and azimuth are shown for squares 1-3 in figure 18, for squares 4-6 in figure 19, and for squares 1-6 in figure 20. As stated previously, because sounding 3 indicated little anisotropy, the program FITELLIPSE by Hart and Rudman (1997) was used to calculate the direction of highest apparent resistivity and the primary fracture strike for each square. Data points that clearly were in error, most likely because of poor electrical connections (shown as dashes in table 1), were dropped from the squares oriented at 350° (square 1) and 5° (squares 4 and 6). In squares 1 and 2, the primary fracture strike is 130° and 114°, respectively. In squares 3-6, the primary fracture strike is 19°, 6°, 12°, and 29°, respectively. The interpreted highest apparent resistivity generally decreased with depth from squares 1-3, but increased from squares 4-6.

Terrain-Conductivity Survey

Data from the terrain-conductivity survey are presented in figure 21. The terrain-conductivity readings decreased as the pipeline and road were crossed, but these changes were within 5 to 6 m. of the pipeline and road. It was concluded from this survey that the presence of the road and the PVC pipeline would not affect the resistivity profiles and soundings anywhere except within that 5- to 6-m distance. This interference, in addition to being unable to block traffic to place electrodes in the entrance road, is the reason for the break in profile lines 1-2, and 3-4 shown in figs. 5 through 10.

Interpretation of Resistivity Profiles and Resistivity Soundings

A comparison of the types and abundance of anomalies along profiles 1 and 3 is presented in figure 11. Because resistivity along profiles 2 and 4 showed little change and probably was affected by buried debris, these profiles were not interpreted. Soundings were interpreted on the basis of graphical results and results from the program FITELLIPSE.

Resistivity Profiles

The pattern of anomalies near 95 m on profile 1 was similar to those at 75 m on profile 3 (fig. 11). In addition, the zone from 35 to 55 m on profile 1 was similar to the zone from 15 to 30 m on profile 3. The offset of these anomalies between profiles 1 and 3 ranged from 20 to 25 m. In addition, on the plot of apparent anisotropy versus distance along the profiles (fig. 6), there were pronounced peaks on profile 1 at 45 m, 80 m, and at 90 m, with a less pronounced peak at 60 m. The peaks on profile 3 were at 20 m, 35 m, 60 m, and 110 m. There may be a structure that
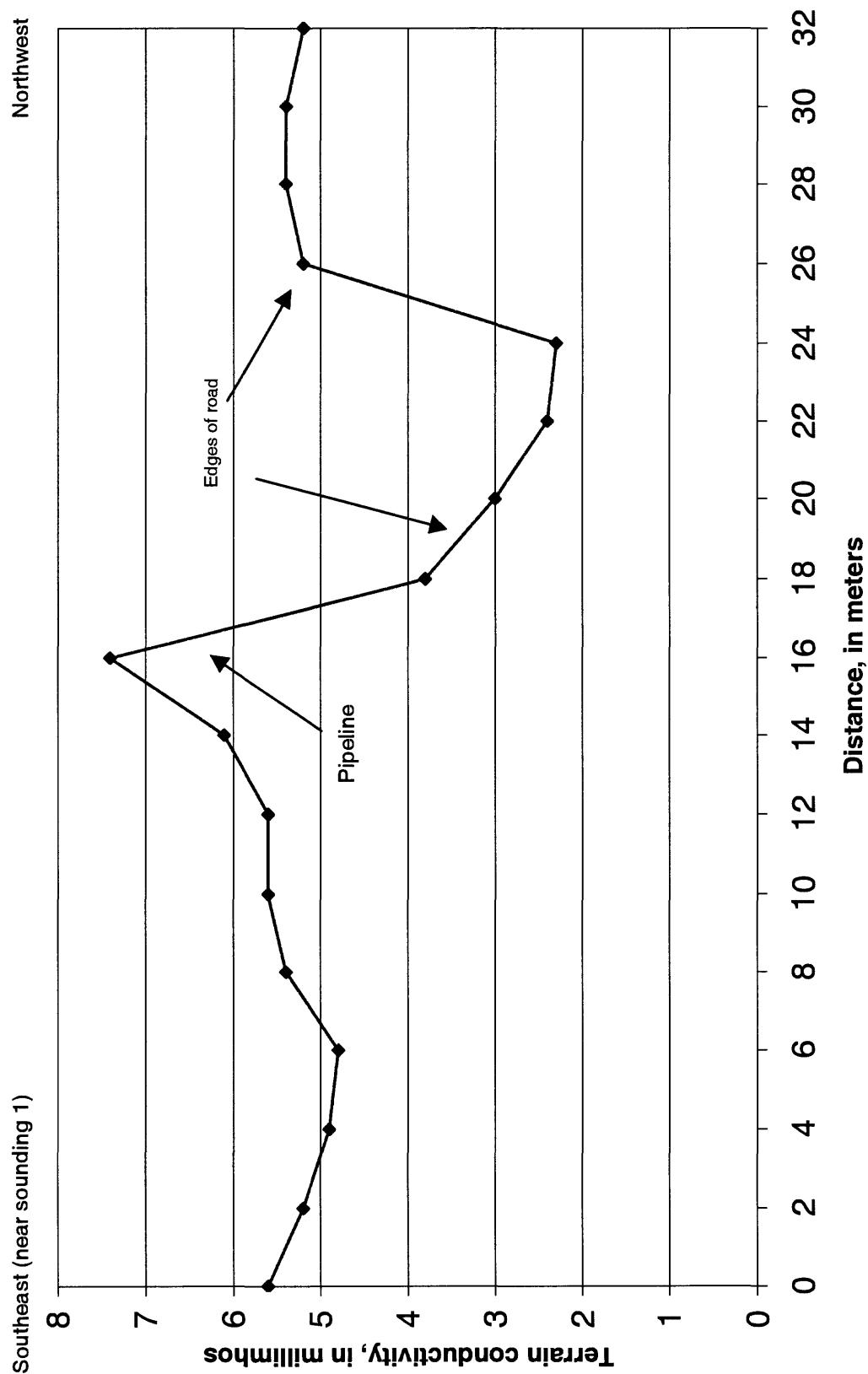
Figure 21. Terrain-conductivity measurements across the gas pipeline and road to the west of sounding 1, Fort Detrick, Maryland.

crosses profiles 1 and 3 at an angle, causing an offset of 20-25 m in the observed peaks on these profiles, assuming that on profile 1, the peaks at 45 m, 60 m, and 80 m matched the peaks on profile 3 at 20 m, 35 m, and 60 m, respectively. There was apparently no match on profile 3 for the peak on profile 1 at 90 m. The peak on profile 3 at 110 m may correlate with a feature in profile 2, where the data are inconclusive. On the basis of a trigonometric solution, an offset of 20 m between profiles 1 and 3 would trend at 77° and an offset of 25 m would trend at 71°. This range of trends for the offset on the anomalies on the profiles fits reasonably closely with the trend of 66° for the fault mapped by Jonas and Stose (1938). As previously described, several Cambrian stratigraphic units are offset along this fault, beginning approximately 1.6 km southwest of the site, with the area of offset continuing over 3.5 km to the southwest along the fault. Cambrian and Precambrian units are offset along this fault to the northeast, beginning approximately 8.8 km northeast of the site.

Resistivity Soundings

At sounding 2, the dominant strike in squares 1-6 was 65° based on the graphical results. The interpreted highest apparent resistivity increased with depth in both sets of squares, ranging from 99 to 309 ohm-meters. This same fracture trend of 65° also was observed in sounding 1, in squares 4-5, based on the graphical results. A possible interpretation is that the fault (66°) is at or very close to the surface at sounding 2, the fault plane dips gently towards sounding 1, and was intersected between squares 2 and 4 on sounding 1, where the most pronounced change in the fracture strike direction occurred (based on graphical and FITELLIPSE results, table 2).

Another fault that trends 131° was mapped by Jonas and Stose (1938) (fig. 2) in the vicinity of profiles 1-4 and soundings 1 and 2. The Frederick Limestone (Cambrian) and the New Oxford Formation (Triassic; red shale and gray to red arkose, with basal limestone conglomerate) contact each other on opposite sides of this fault. This 131° fault trend is close to the graphical trend of 110° observed in sounding 1, square 1. The field site is within 0.4 km of the mapped intersection of this fault with the fault that trends 66°. A possible interpretation based on the graphical solution is that the fracture orientation in the shallower bedrock observed in square 1 of sounding 1 may be influenced by the fault that trends 131° and the deeper bedrock observed in squares 4-6 of sounding 1 may be influenced by the fault that trends 66°. The FITELLIPSE results indicate that the major change in fracture strike orientation occurred between squares 2 and 4. Soundings 1 and 2, therefore, may have been very close to the intersection of these faults.

The data are consistent with the presence of a fault (or unconformity) that trends 66° between soundings 1 and 2. Based on the graphical solution, the dominant fracture direction in all 6 squares on sounding 2 was 65°. On sounding 1, the graphical solution for square 1 was that the dominant fracture direction was 110°, which may have been influenced by the nearby fault trending at 131°. The FITELLIPSE program showed the dominant fracture direction in square 1 at 107°. The graphical solution for square 2 was 95° and the FITELLIPSE solution was 97°. The graphical solution showed squares 4-6 at 65°, 65°, and 50°, respectively. The FITELLIPSE solution showed square 3 at 19° and it showed squares 4-6 at 50°, 62°, and 62°, respectively. This solution indicates that soundings 1 and 2 may have been near the intersection of the faults trending 66° and 131° shown on figure 2. It also is likely that the fault trending 66° dips from sounding 2 towards sounding 1, where the fault was encountered at depths represented between

squares 2 and 4. The dip on the surface of the unconformity in the area is estimated to be about 20° (ICF Kaiser Engineers, 1998), which corresponds to the dip of the Triassic units (Nutter, 1975) deposited on the surface of the unconformity.

According to John Lane (U.S. Geological Survey, oral commun., 1998), the maximum depth of penetration for a square is equal to the length of its side, but the depth of penetration usually is less and can be affected by the resistivities of the various layers, which are affected by porosity, water content, water quality, and the rock matrix. Square 2 on sounding 1 would have a maximum depth of penetration of 7.07 m. Square 4 on sounding 1 would have a maximum depth of penetration of 14.14 m. The distance between the centerpoints of sounding 1 and 2 was 60 m. Assuming that the fault is at the surface at sounding 2, the dip would range from 6.7° to 13.3°, which is relatively close to the true dip of 20° estimated by ICF Kaiser Engineers (1998).

Based on the FITELLIPSE results, sounding 3 in squares 1 and 2 showed a fracture strike direction of 130° and 114°, respectively. Squares 3 through 6 showed fracture strike directions of 19°, 6°, 12°, and 29°, respectively. In addition, the interpreted highest apparent resistivities ranged from 275 to 572 ohm-meters, which is a slightly broader range (297 ohm-meters) than that observed at soundings 1 (229 ohm-meters) and 2 (210 ohm-meters). The site for sounding 3 was selected to collect background information on the Frederick Limestone away from the suspected fault or unconformity. Using a program by Zohdy and Bisdorf (1989) that uses mean resistivity values to calculate the resistance of the bedrock, it was determined that soundings 1 and 2 were on resistive bedrock (greater than 1,000 ohm-meters) and sounding 3 was on less resistive bedrock (200 ohm-meters). The site for sounding 3 was in an area where solution cavities have been encountered. If solution channels are present in the area, they may have caused the slightly broader range observed in the apparent resistivity and may have influenced the observed fracture strike directions.

Summary and Conclusions

A suspected geologic structure crosses Area B near the eastern boundary of Fort Detrick, near Frederick, Maryland. If this structure is present, there is some concern that ground-water contaminants may be migrating along it. If so, this structure might provide an ideal site to install an extraction well to intercept contaminants before they can migrate beyond the base boundary. The U.S. Geological Survey, in cooperation with the Baltimore District of the U.S. Army Corps of Engineers, performed azimuthal square-array direct-current resistivity surveys at Fort Detrick to determine if there was geophysical evidence of the suspected structure. Four square-array profiles and three soundings were performed from July 8 through 13, 1998.

The area where the profiles and soundings were performed was selected because geologic structures have been mapped in the vicinity by several previous investigators. In addition, the field site is adjacent to the base boundary near a large spring. Because the area is an open grassy field with minimal cultural interferences such as powerlines or buried utilities, it was suitable for working with the electrodes and electrical cables necessary for this geophysical technique. The resistivity surveys were performed to answer specific questions about the suspected geologic structure. These questions and their answers are summarized below.

• What is the fracture orientation in the near-surface bedrock?

The dominant fracture orientation in sounding 1, square 1 (maximum depth of penetration is 4.24 m (meters)) was 110° (degrees) based on the graphical solution. For sounding 1, square 2 (maximum depth of penetration is 7.07 m), it was 95°, also based on the graphical solution. In sounding 2, the dominant fracture orientation in squares 1 and 2 using the graphical solution was 65°.

• Is there an apparent change in fracture orientation in the near-surface bedrock and with depth?

In sounding 1, based on the graphical solution, the fracture orientation in the shallower bedrock observed in squares 1 and 2 (110° and 95°, respectively) shifted to a range of 50° to 65° in squares 3-6. On the basis of the graphical solution, no change in fracture orientation in the near-surface bedrock or with depth was observed among the squares in sounding 2.

• Is there evidence of a structure based on changes in primary and secondary fracture orientations?

The field site is within 0.4 kilometers of the intersection of an earlier mapped fault trending 131° with a fault trending 66°. The shift in fracture orientation between squares 1 and 2 on sounding 1 (110° and 95°, respectively) to a range of 50° to 65° in squares 3-6 indicates that the uppermost 2 squares may have been affected by the fault trending 131°, and the deeper squares (3-6) may have been affected by the fault trending 66°.

• If there is a structure, can preliminary information on its depth be determined?

The FITELLIPSE program results indicate that the major change in strike occurred between squares 2 and 4 on sounding 1, at maximum depths of approximately 7 to 14 meters.

• If there is a structure, how closely can it be located?

Soundings 1 and 2 may have been near the intersection of the faults trending 66° and 131°. It is likely that the fault (unconformity) trending 66° dips from sounding 2 towards sounding 1, where it was encountered at depths represented between squares 2 and 4. Assuming the fault is at the surface at sounding 2, and that the maximum depth of penetration of square 2 was 7.07 meters and of square 4 was 14.14 meters, the dip of the fault would range from 6.7° to 13.3°, which is relatively close to the dip of 20° estimated in an earlier study of the unconformity. In addition, the trend of 71°-77° for the offset on the anomalies on profiles 1 and 3 is consistent with the trend of 66° for the earlier mapped fault.

References Cited

Cleaves, E.T., Edwards, J.R., and Glaser, J.D., compilers, 1968, Geologic map of Maryland: Maryland Geological Survey, 1 sheet, scale 1:250,000.

Cloos, Ernst, 1941, Flowage and cleavage in Appalachian folding: N.Y. Academy of Science Transactions, series 2, v. 3, p. 185-190.

_____, 1947, Oolite deformation in the South Mountain fold, Maryland: Bulletin of the Geological Society of America, v. 58, p. 843-917.

Duigon, M.T., and Dine, J.R., 1987, Water resources of Frederick County, Maryland: Maryland Geological Survey Bulletin 33, 106 p., 2 pls.

Habberjam, G.M., 1972, The effects of anisotropy on square array resistivity measurements: Geophysical Prospecting, v. 20, p. 249-266.

_____, 1979, Apparent resistivity observations and the use of square array techniques, in Saxov, S. and Flathe, H. (eds.): Geoexploration Monographs, series 1, no. 9, p 1-152.

Hart, D., and Rudman, A.J., 1997, Least-squares fit of an ellipse to anisotropic polar data: application to azimuthal resistivity surveys in karst regions: Computers and Geosciences, v. 23, p. 189–194.

ICF Kaiser Engineers, 1998, Draft document: Fort Detrick remedial investigation of Area B, volumes 1, 2, and 3: Edgewood, Maryland, ICF Kaiser Engineers, [variously paged].

Jonas, A.I., and Stose, G.W., 1938, Geologic map of Frederick County and adjacent parts of Washington and Carroll Counties: Maryland Geological Survey, scale 1:62,500, 1 sheet.

Lane, J.W., Jr., Haeni, F.P., and Watson, W.M., 1995, Use of a square-array direct-current resistivity method to detect fractures in crystalline bedrock in New Hampshire: Ground Water, v. 33, no. 3, p. 476- 485.

Lewis, M.R., and Haeni, F.P., 1987, The use of surface geophysical techniques to detect fractures in bedrock—an annotated bibliography: U.S. Geological Survey Circular 987, 14 p.

Nutter, L.J., 1973, Hydrogeology of the carbonate rocks, Frederick and Hagerstown Valleys, Maryland: Maryland Geological Survey Report of Investigations No. 19, 70 p., 2 pl.

_____, 1975, Hydrogeology of the Triassic rocks of Maryland: Maryland Geological Survey Report of Investigations No. 26, 37 p.

Reinhardt, Juergen, 1974, Stratigraphy, sedimentology and Cambro-Ordovician paleogeography of the Frederick Valley, Maryland: Maryland Geological Survey Report of Investigations No. 23, 74 p, 2 pl.

U.S. Army Corps of Engineers, 1983, Study of proposed landfill Area B, Fort Detrick, Maryland: Baltimore, Maryland, U.S. Army Corps of Engineers Baltimore District, 18 p.

Whitaker, J.C., 1955, Geology of Catoctin Mountain, Maryland and Virginia: Bulletin of the Geological Society of America, v. 66, p. 435-462

Zohdy, A.A.R., and Bisdorf, R.J., 1989, Programs for the automatic processing and interpretation of Schlumberger sounding curves in QuickBASIC 4.0: U.S. Geological Survey Open-File Report 89-0137-A, 64 p.

APPENDIX A

Reprinted with permission of the National Ground Water Association, copyright 1995, all rights reserved.

Use of a Square-Array Direct-Current Resistivity Method to Detect Fractures in Crystalline Bedrock in New Hampshire

by J. W. Lane, Jr., F. P. Haeni, and W. M. Watson[a]

Abstract

Azimuthal square-array direct-current (dc) resistivity soundings were used to detect fractures in bedrock in the Mirror Lake watershed in Grafton County, New Hampshire. Soundings were conducted at a site where crystalline bedrock underlies approximately 7 m (meters) of glacial drift. Measured apparent resistivities changed with the orientation of the array. Graphical interpretation of the square-array data indicates that a dominant fracture set and (or) foliation in the bedrock is oriented at 030° (degrees). Interpretation of crossed square-array data indicates an orientation of 027° and an anisotropy factor of 1.31. Assuming that anisotropy is due to fractures, the secondary porosity is estimated to range from 0.01 to 0.10.

Interpretations of azimuthal square-array data are supported by other geophysical data, including azimuthal seismic-refraction surveys and azimuthal Schlumberger dc-resistivity soundings at the Camp Osceola well field. Dominant fracture trends indicated by these geophysical methods are 022° (seismic-refraction) and 037° (dc-resistivity). Fracture mapping of bedrock outcrops at a site within 250 m indicates that the maximum fracture-strike frequency is oriented at 030°.

The square-array dc-resistivity sounding method is more sensitive to a given rock anisotropy than the more commonly used Schlumberger and Wenner arrays. An additional advantage of the square-array method is that it requires about 65 percent less surface area than an equivalent survey using a Schlumberger or Wenner array.

Introduction

Research on the application of surface-geophysical methods to detect bedrock fractures and to estimate hydraulic properties of fractured bedrock is being conducted by the U.S. Geological Survey (USGS) as part of a bedrock research investigation in the Mirror Lake watershed of the Hubbard Brook Experimental Forest in Grafton County, New Hampshire (Figure 1).

One part of the study assesses the ability of direct-current (dc) resistivity methods to detect bedrock fractures. Dc-resistivity methods have been successfully used by a number of investigators to detect bedrock fractures (Risk, 1975; McDowell, 1979; Palacky et al., 1981; Soonawala and Dence, 1981; Taylor, 1982; Mallik et al., 1983; Leonard-Mayer, 1984a, 1984b; Ogden and Eddy, 1984; Taylor, 1984; Taylor and Fleming, 1988; Lieblich et al., 1991, 1992; Ritzi and Andolsek, 1992). Most of these investigations have used collinear arrays (Wenner or Schlumberger) rotated about a fixed centerpoint to measure azimuthal variations in apparent resistivity that are related to sets of similarly oriented, steeply dipping fractures (Lewis and Haeni, 1987).

Habberjam (1972) showed that a square array is more sensitive to anisotropy in the subsurface and requires less surface area than collinear arrays. Recently, dc-resistivity surveys using a square array have been conducted to detect productive fracture zones in crystalline bedrock for ground-water supply (Darboux-Afouda and Louis, 1989; Sehli, 1990). These studies verified Habberjam's earlier work, showing that the square array has a greater sensitivity to a given bedrock anisotropy and requires less surface area than collinear arrays.

The square array was tested at the Mirror Lake research site. This paper describes the square-array dc-resistivity method, outlines a simplified method of data analysis to determine fracture strike and secondary porosity, and presents the results of the field test.

The Square-Array Method

The square array was originally developed as an alternative to Wenner or Schlumberger arrays when a dipping subsurface, bedding, or foliation was present (Habberjam and Watkins, 1967). A complete discussion of the square array and methods of data analysis is provided by Habberjam (1979). Techniques for analyzing directional-resistivity data provided by the square-array method have been developed (Habberjam, 1972), but the method has not been widely used. Few case studies or interpretive methods specifically applied to the square array are found in the literature, although commercial software is available for layered earth interpretations.

39
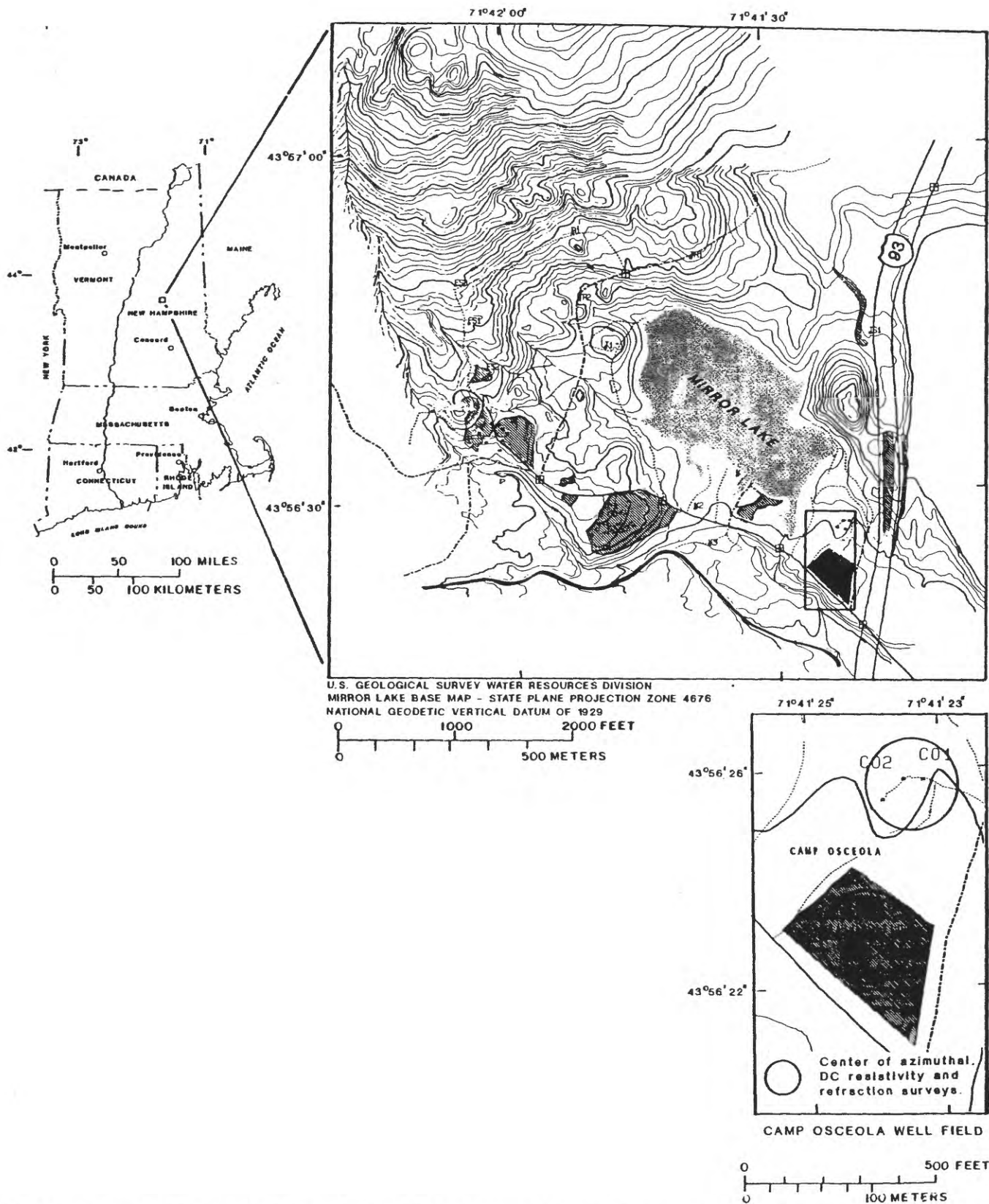
Fig. 1. Location of U.S. Geological Survey fractured bedrock research site, showing square-array test area, Mirror Lake, Grafton County, New Hampshire. (Modified from Haeni et al., 1993, fig. 1.)

Field Measurements

A dc-resistivity survey using the square-array method is conducted in a manner similar to that for traditional collinear arrays. The location of a measurement is assigned to the centerpoint of the square. The array size (A) is the length of the side of the square. The array is expanded symmetrically about the centerpoint, in increments of $A(2)^{1/2}$ (Habberjam and Watkins, 1967), so that the sounding can be interpreted as a function of depth.

For each square, three measurements are made—two

Starting orientation

Second orientation
rotated 45 degrees
about center point

Current electrode configuration
for Crossed Square array

Alpha	1 - 4	=	Pa_1
Alpha'	5 - 8	=	Pa_2
Beta	1 - 2	=	Pa_3
Beta'	5 - 6	=	Pa_4
Gamma	1 - 3		
Gamma'	5 - 7		

Electrode configurations per Square array
AB = Current electrodes
MN = Potential electrodes

Fig. 2. Electrode positions for square-array measurements.

perpendicular measurements (alpha, α; and beta, β) and one diagonal measurement (gamma, γ) (Figure 2). The α and β measurements provide information on the directional variation of the subsurface apparent resistivity (ρ_a). The azimuthal orientation of the α and β measurements is that of the line connecting the current electrodes. The γ measurement serves as a check on the accuracy of the α and β measurements.

In an isotropic medium,

$$\rho_{a\alpha} = \rho_{a\beta}, \text{ therefore, } \rho_{a\gamma} = 0, \text{ and} \quad (1)$$

in a homogeneous anisotropic medium,

$$\rho_{a\gamma} = \rho_{a\alpha} - \rho_{a\beta}, \quad (2)$$

where ρ_a = apparent resistivity, in ohmmeters.

Apparent resistivity is determined using the equation:

$$\rho_a = \frac{K\Delta V}{I}, \quad (3)$$

where ρ_a = apparent resistivity; K = geometric factor for the array; ΔV = potential difference, in volts; and I = current magnitude, in amperes.

For the square array,

$$K = \frac{2\pi A}{2 - (2)^{1/2}}, \text{ (Habberjam and Watkins, 1967)} \quad (4)$$

where A = square-array side length, in meters. In practice, multiple square-array data are collected at small angular intervals. For example, six square arrays separated by a rotational angle of 15° will provide three independent crossed square-array data sets (two square arrays separated

by an angle of 45°; Figure 2) for analysis, as well as sufficient data for graphical display and interpretation of individual square-array data on a rosette diagram using Taylor and Fleming's methods (1988).

Data Analysis

The data were analyzed using a method described by Habberjam (1972). The following discussion is a brief summary of the method and outlines the potential uses of the square-array method for hydrologic investigations.

Depth Sounding

Habberjam and Watkins (1967) demonstrated that apparent-resistivity data obtained with a square array can be interpreted using published methods for Wenner or Schlumberger soundings. This is done by translating apparent-resistivity data obtained from the square array to those of equivalent Wenner or Schlumberger arrays.

First, the square-array resistivity measurements are reduced to a single measurement (ρ_m) by

$$\rho_m = [(\rho_{a\alpha})(\rho_{a\beta})]^{1/2}, \text{ Habberjam and Watkins, 1967 } (5)$$

where ρ_m = mean geometric resistivity.

The more rigorous relation between the size of a square array and the size of an equivalent Wenner or Schlumberger array is given by

$$A = r\left[\frac{2(r + s)}{2r + s} \right], \quad (6)$$

where A = square-array side length, in meters; r = AM = current electrode and nearest potential electrode separation;
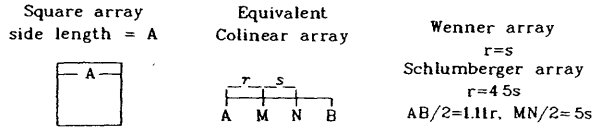
478

41

Fig. 3. Common collinear arrays equivalent to a square array of side length A.

and $s = MN$ = potential electrode separation (Figure 3).

Later work (Habberjam, 1972) showed that an azimuthal-independent value for that spacing can be obtained by calculating the geometric mean of ρ_m obtained from two square arrays separated by a rotational angle of 45° (about the centerpoint) (the crossed square array). However, reduction of the square-array resistivity measurements to yield a single directionally stable measurement for layered earth interpretation removes the information about directional resistivity differences contained within the individual square-array measurements.

Azimuthal Resistivity

Variations in azimuthal resistivity can be caused by many factors such as slope of the bedrock surface, or dip of bedding or foliation. Experiments by Sauck and Zabik (1992) have shown that azimuthal resistivity data can be affected by overburden thickness. The following discussion assumes that the resistivity differences are only caused by similarly oriented, steeply dipping fractures (Figure 4).

Habberjam (1972) derived the expression for the variation of apparent resistivity with square-array orientation over a homogeneous anisotropic earth. For fractured rock that approximates such a medium, the predicted square-array apparent resistivity in a given orientation is

$$\rho_a = \frac{\rho_m}{2 - (2)^{1/2}} \left(\frac{2}{[1 + (N^2 - 1)\cos\theta^2]^{1/2}} \right) -$$

$$\left(\frac{1}{[2 + (N^2 - 1)(1 + \sin2\theta)]^{1/2}} \right) -$$

$$\left(\frac{1}{[2 + (N^2 - 1)(1 - \sin2\theta)]^{1/2}} \right), \qquad (7)$$

where $\rho_m = [(\rho_{a_t})(\rho_{a_l})]^{1/2}$; ρ_{a_t} = apparent resistivity perpendicular to fractures; ρ_{a_l} = apparent resistivity parallel to fractures; θ = angle measured from azimuth of current electrodes to fracture strike; N = effective vertical anisotropy, $= [(1 + (\lambda^2 - 1)\sin\alpha^2)]^{1/2}$; λ = coefficient of anisotropy; $\lambda = (\rho_{a_t}/\rho_{a_l})^{1/2}$; α = dip of fractures; $N = \lambda$ for $\alpha = \pi/2$.

When variations in azimuthal resistivity are detected over an anisotropic earth, and the variations are caused by fractures, the interpretive methods of Habberjam (1972; 1975) and Taylor (1984) can be used to determine fracture strike and to estimate secondary porosity.

Determination of Fracture Strike

The fracture strike can be determined graphically or analytically. To interpret strike graphically, the apparent resistivity for azimuthal square arrays is plotted against the azimuth of that measurement. The principal fracture strike direction is perpendicular to the direction of maximum resistivity.

Crossed square-array data can be interpreted analytically in order to yield fracture strike (Habberjam, 1975):

$$\theta = \frac{1}{2} \tan^{-1}\left[\frac{(D^{-2} - C^{-2})}{(A^{-2} - B^{-2})} \right], \qquad (8)$$

where θ = fracture strike, measured from ρ_{a_1};
$A = [(\rho_{a_3} + 3\rho_{a_1})/2 + (\rho_{a_4} + \rho_{a_2})/(2)^{1/2}]/[(2 + (2)^{1/2}];$
$B = [(\rho_{a_1} + 3\rho_{a_3})/2 + (\rho_{a_2} + \rho_{a_4})/(2)^{1/2}]/[(2 + (2)^{1/2}];$
$C = [(\rho_{a_4} + 3\rho_{a_2})/2 + (\rho_{a_1} + \rho_{a_3})/(2)^{1/2}]/[(2 + (2)^{1/2}];$
and
$D = [(\rho_{a_2} + 3\rho_{a_4})/2 + (\rho_{a_3} + \rho_{a_1})/(2)^{1/2}]/[(2 + (2)^{1/2}];$
$\rho_{a_1}, \rho_{a_2}, \rho_{a_3}$, and ρ_{a_4} are constituent resistivity measurements from a crossed square array (Figure 2).

Estimation of Secondary Porosity

Using the crossed square-array measurements, the secondary porosity (ϕ) can be estimated by modifying Taylor's method developed for collinear arrays in saturated, clay-free, nonshale rocks (1984). To calculate secondary porosity, it is first necessary to calculate the anisotropy (N) from the field data, using Habberjam's method (1975):
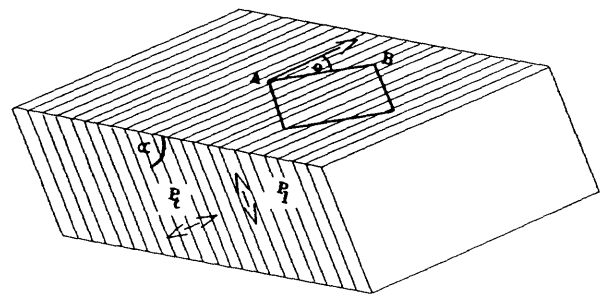
$$N = [(T + S)/(T - S)]^{1/2}, \qquad (9)$$

where $T = A^{-2} + B^{-2} + C^{-2} + D^{-2}; S = 2[(A^{-2} - B^{-2})^2 + (D^{-2} - C^{-2})^2]^{1/2};$ and A, B, C, and D are defined previously. The secondary porosity is then estimated by:

$$\phi = \frac{3.41 \times 10^4(N - 1)(N^2 - 1)}{N^2 C(\rho_{max} - \rho_{min})}, \qquad (10)$$

where ϕ = secondary porosity; ρ_{max} = maximum square-array apparent resistivity; ρ_{min} = minimum square array apparent resistivity; and C = specific conductance of ground water in microsiemens per centimeter.

EXPLANATION

P_l = resistivity parallel to fracturing
P_t = resistivity perpendicular to fracturing
θ = angle from fracture strike to current electrodes AB
α = angle of fracture dip

Fig. 4. Model of homogeneous anisotropic Earth. (Modified and reprinted from Habberjam, 1972, fig. 2, and published with permission.)

Comparison of Square Array and Collinear Array Sensitivity to Anisotropy

To correctly interpret azimuthal dc-resistivity data over fractured rock, the bedrock must behave as an anisotropic medium. Satisfying this requires the electrode spacings to be large with respect to the fracture spacing (Taylor, 1982). The square array has a ratio of potential electrode to current electrode spacing of 1:1. The Wenner array ratio is 1:3, and the Schlumberger ratio is generally less than 1:10. As the above arrays are expanded, the square array, with the largest electrode-spacing ratio, will most rapidly satisfy the above condition.

The square array has been shown to be more sensitive to anisotropy than the Schlumberger or Wenner array (Habberjam, 1972; LeMasne, 1979; Darboux-Afouda and Louis, 1989). For the square array, the ratio of apparent resistivity measured perpendicular to fracture strike ($\rho_{a\perp}$) to apparent resistivity parallel to fracture strike ($\rho_{a\parallel}$) is called the apparent anisotropy (λ_a) and is given by the ratio:

$$\lambda_a = \frac{\rho_{a\perp}}{\rho_{a\parallel}} = \frac{N[(N^2 + 1)^{1/2} - 1]}{[(N^2 + 1)^{1/2} - N]},$$

(Darboux-Afouda and Louis, 1989)   (11)

The apparent anisotropy for the Schlumberger or Wenner array is given by:

$$\lambda_a = \frac{\rho_{a\parallel}}{\rho_{a\perp}} = N \qquad (12)$$

where N = effective vertical anisotropy.

The apparent anisotropy of the square array and the Schlumberger array for a true rock anisotropy is shown in Figure 5. The higher apparent anisotropy measured by the
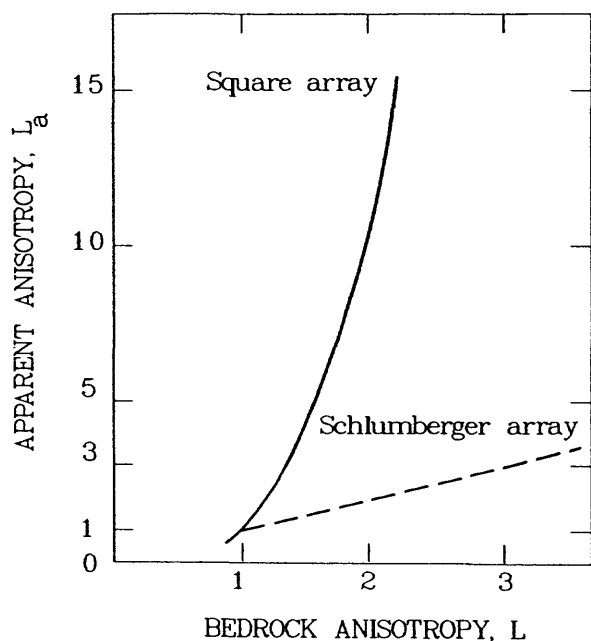

Fig. 5. Anisotropy measured by the square array and the Schlumberger array for a given bedrock anisotropy. (Reprinted from Darboux-Afouda and Louis, 1989, fig. 2 and published with permission.)

square array is an advantage, because the anisotropy is less likely to be obscured by heterogeneities in bedrock or over-burden, bedrock relief, cultural noise, electrode placement errors, or other sources of noise.

Survey Area Requirements

The square-array geometry is more compact than Schlumberger or Wenner arrays for azimuthal surveys. The square array requires 65 percent less surface area than the equivalent collinear arrays (Habberjam and Watkins, 1967). This is an advantage in an area with significant lateral heterogeneities or when the area available to conduct a survey is limited.

Maximum Resistivity in Relation to Fracture Strike

The direction of maximum apparent resistivity measured by the square array will be perpendicular to fracture strike. This is a function of the cosine term in the denominator of equation (7).

The direction of maximum apparent resistivity measured by the collinear array will be parallel to the fracture strike (Habberjam, 1972). This is a consequence of the "paradox of anisotropy" (Keller and Frischknecht, 1966) and is determined by the sine term in the denominator of the following equation showing apparent resistivity in relation to orientation:

$$\rho_a(\theta) = \frac{K \Delta V}{I} = \frac{\rho_m}{[[1 + (N^2 - 1) \sin\theta^2]]^{1/2}}, \qquad (13)$$

where K = geometric factor for the array; N = effective vertical anisotropy; and ρ_m = mean geometric resistivity.

Use of Square Array to Detect Fractures at Grafton County, New Hampshire

The square-array dc-resistivity method was field tested in Priest Field, near the Camp Osceola (CO) well cluster, located at the Mirror Lake research site (Figure 1). At this site, approximately 7 m (meters) of stratified glacial drift is underlain by crystalline bedrock.

The square-array survey was conducted during the Summer of 1992. The survey consisted of six square-array soundings separated by a 15° rotational angle about the array centerpoint. The A-spacings of the arrays were expanded from 5 m to 50 m [in increments of $(2)^{1/2}$] for each sounding. The data were collected using an ABEM Multimac dc-resistivity system. (Use of tradenames is for identification purposes only and does not constitute endorsement by the U.S. Geological Survey.) This computer-controlled data acquisition and storage system (Figure 6) allowed a complete sounding at a given azimuth to be collected automatically through remotely accessed addressable switchers, which connected electrodes for a given measurement. Software provided with the system was modified for the square array to control the measurement sequence.

Interpretation of Square-Array Data and Crossed Square-Array Data

Data collected in Priest Field show a significant variation of apparent resistivity for different azimuthal array

480

43

Table 1. Azimuthal Apparent Resistivities Collected at Priest Field, Mirror Lake Watershed, New Hampshire

A-spacing (meters)	Geometric factor (K)	Mean	Square-array azimuthal apparent resistivities, in ohmmeters											
			0	15	30	45	60	75	90	105	120	135	150	165
5	53.6	7,380	6,790	6,870	7,417	7,044	7,129	7,514	7,991	8,141	7,535	7,385	—	7,374
7.1	75.8	7,604	7,023	6,932	7,538	7,504	7,561	8,183	8,388	8,449	7,546	7,197	—	7,326
10	107.3	7,030	5,859	6,073	6,320	6,218	6,824	7,275	7,854	7,758	7,146	6,985	6,975	6,374
14.1	151.7	5,149	4,885	4,475	4,369	4,392	4,809	5,067	5,476	6,129	5,810	5,810	5,613	4,961
20	214.5	3,628	3,696	3,389	3,087	2,969	3,179	3,314	3,376	3,700	4,030	4,232	4,138	3,762
28.3	303.4	2,479	2,555	2,348	2,112	2,040	2,057	2,148	2,209	2,558	2,894	3,004	3,167	2,661
40	429.0	1,987	1,707	1,167	1,347	1,418	1,700	1,806	2,068	2,561	2,831	2,664	2,561	1,913
50	536.3	1,911	1,341	1,148	1,132	1,279	1,877	1,845	1,866	2,944	3,040	2,660	2,328	1,480

— No data available.

orientations for all A-spacings. Apparent-resistivity data collected at the site are shown in Table 1. The data from the largest arrays were analyzed to minimize possible overburden effects. The apparent resistivities plotted against azimuth are shown for the 40- and 50-m A-spacings, which are least affected by the overburden (Figure 7). For both A-spacings shown, the maximum resistivity measured is parallel to a trend of 120°. A graphical interpretation of the data is that a primary fracture set is present with a strike of 030°. The 50-m data show a secondary trend of high resistivity at 060°. Assuming that these data do not reflect heterogeneities in the bedrock, this peak could indicate the presence of a secondary fracture set oriented at 150°.

Because data for six square arrays separated by 15° were collected, there are three independent crossed square arrays available for analysis. Using the analytical methods described in the section "Field Measurements" for the 50-m data, a strike estimate of 027° and an anisotropy value of 1.31 was obtained.

Using these analytical results for the strike and anisotropy values, the apparent resistivity values predicted using equation (6) were calculated and the results superimposed

on the field data (Figure 7). This shows that the field data closely approximate the data for an isotropic homogeneous earth.

Using the anisotropy of 1.31, a maximum resistivity of 3,040 ohm-m (ohmmeters), a minimum resistivity of 1,132 ohm-m, and a range of specific conductance for ground water in the CO well field of 30 to 315 $\mu S/cm$ (P. T. Harte, U.S. Geological Survey, written commun., 1991), and equation (10), the secondary porosity due to fracturing is estimated to range from 0.01 to 0.10. This demonstrates the sensitivity of the secondary porosity estimate to the specific conductance of ground water.

Comparison of Interpreted Data and Other Supporting Data
Fracture Strike

An outcrop located on the center median of Interstate 93 (within 250 m of the site) consists of schist, massive granitic dikes, granitic dikes with schist xenoliths, and pegmatite (C. C. Barton, U.S. Geological Survey, written commun., 1989). The graphically interpreted fracture-strike from the square-array data of 030° and the crossed square-array data of 027° correlates with fracture-strike frequency data measured at the I-93 outcrop. Analysis of the measured fracture-strike data yields a mean fracture-strike frequency maximum of 030° with major peaks at 005° and 040°. Most of the fractures are steeply dipping (C. C. Barton, U.S. Geological Survey, written commun., 1993; Figure 8). The secondary resistivity maximum seen in the 50-m square-array data indicates the possible presence of another fracture set oriented at 150°. This might correlate with a minor fracture strike maximum at the outcrop oriented at 135° or indicate a change in foliation orientation.

Azimuthal p-wave seismic-refraction surveys have been conducted at the square-array test site (Lieblich et al., 1991). Data were collected every 22.5° about the same centerpoint used in the square-array survey. The contrast between the measured seismic velocity and the refraction-line orientation (Figure 9) was interpreted as indicating a fracture and (or) foliation oriented at 022.5° (Lieblich et al., 1991).

An azimuthal dc-resistivity survey using the Schlumberger array was conducted at the CO well field 100 m from the square-array test site (Haeni et al., 1993). Data were collected every 45° with a Bison 2390 resistivity system,
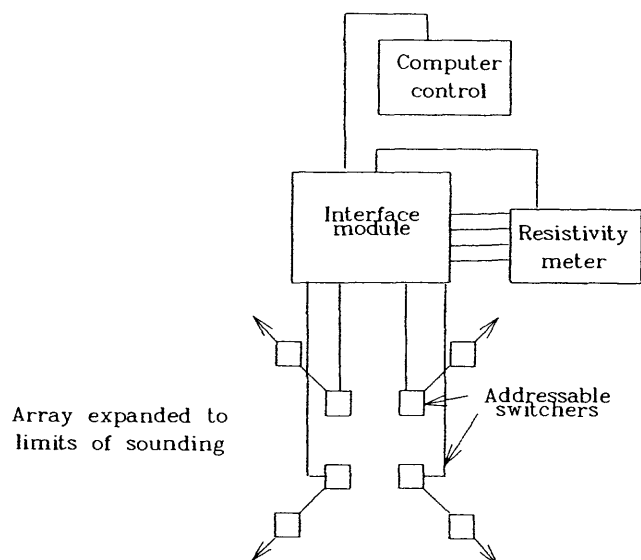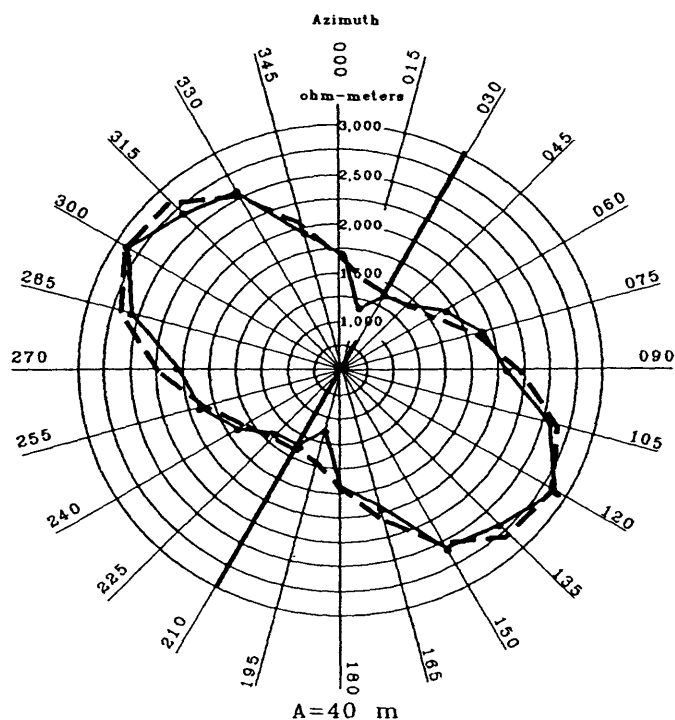

Fig. 6. Block diagram of direct-current resistivity data-collection system.

Azimuth

A=40 m

Azimuth

A=50 m

EXPLANATION

⌒1000⌒ Line of equal apparent resistivity,
         in ohm meters

━━━━━ Interpreted primary fracture strike

• • • • • Possible secondary fracture strike

━ ━ Forward modeled data for homogeneous
     anisotropic earth

•   Data points showing apparent resistivity
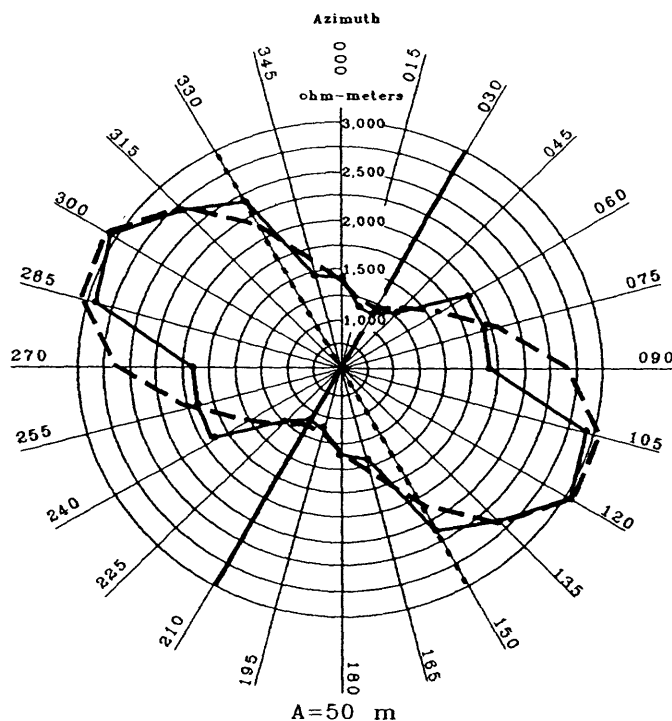   at indicated azimuthal directions

000 Compass azimuth, in degress

Fig. 7. Square-array apparent resistivity plotted against azimuth for the 40- and 50-meter A-spacings, collected at Priest Field, U.S. Geological Survey fractured bedrock research site, Mirror Lake, New Hampshire. (Modified from Haeni et al., 1993, fig. 5).

and the AB/2 spacing was expanded from 3 m to 30 m. Qualitative analysis of these data support a fracture set and (or) foliation oriented at 037° (Figure 10); however, the anomalously large anisotropy indicates some cultural interference (for example, well casing or buried metal) within the data.

Two azimuthal surveys using the Schlumberger array also were conducted at the square-array test site about the same centerpoint as the square array. One set of soundings

was conducted every 22.5° using a Bison 2390 resistivity system. The AB/2 spacings were expanded from 3 m to 40 m. A second set of soundings was conducted every 15° with the ABEM Multimac system. The AB/2 spacings were expanded from 3 m to 40 m. The fracture orientation interpreted from each of these data sets is 352° (Figure 11).

Inspection of the data, field site, and survey design may explain the discrepancy between the Schlumberger and square-array data, and illustrate possible weaknesses of
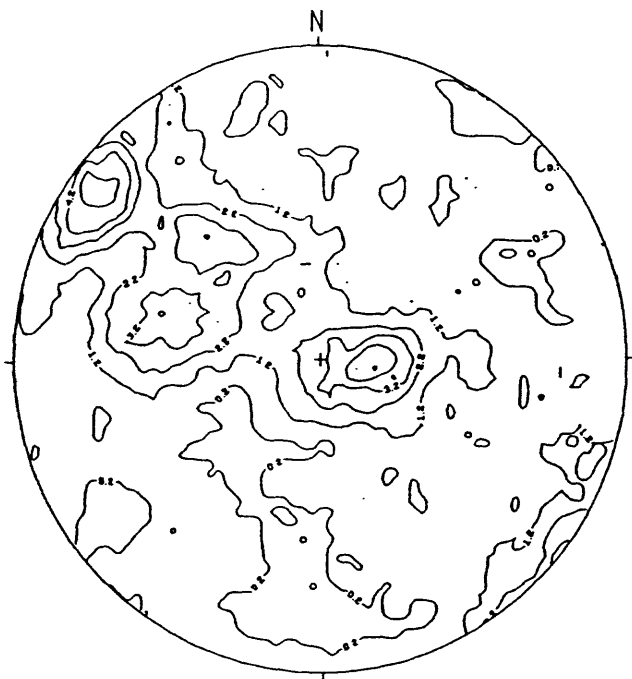
45

Fig. 8. Equal area plot of fractures mapped from Route I-93 outcrops near the U.S. Geological Survey fractured bedrock research site, West Thornton, New Hampshire. (From C. C. Barton, U.S. Geological Survey, written commun., 1993.)

azimuthal Schlumberger array surveys for fracture detection at this site. Because the large current electrode separation of the Schlumberger array required a large surface area, a buried phone line was included within the array. This phone line was not located within the square array survey area. The largest MN/2 potential-electrode separations used for the Schlumberger array was 4 m, which may not have satisfied the theoretical requirement of large electrode spacing as a function of fracture spacing. In addition, heterogeneities present near potential electrodes may have affected the Schlumberger data. In view of the above, the square-array results are interpreted to indicate fracture conditions at the test site more accurately than the Schlumberger array results.

Secondary Porosity

The secondary porosity estimate interpreted from the 50-m data ranges from .01 to .1. This range encompasses values higher than average secondary porosities for crystalline rock, which are generally less than 0.02 (Freeze and Cherry, 1979). An estimate of the fracture porosity at well CO-1, made by measuring the number of fractures and the average fracture aperture, is 0.001 (P. T. Harte, U.S. Geological Survey, oral commun., 1992). A reason for this difference is that secondary porosity estimates obtained from wells are sensitive to subhorizontal fractures and the dc-resistivity method is more sensitive to vertical fractures. Another explanation is that foliation could be a significant contributor to anisotropy. The secondary porosity calculations from the square array assumed that fracturing is the only cause of anisotropy.
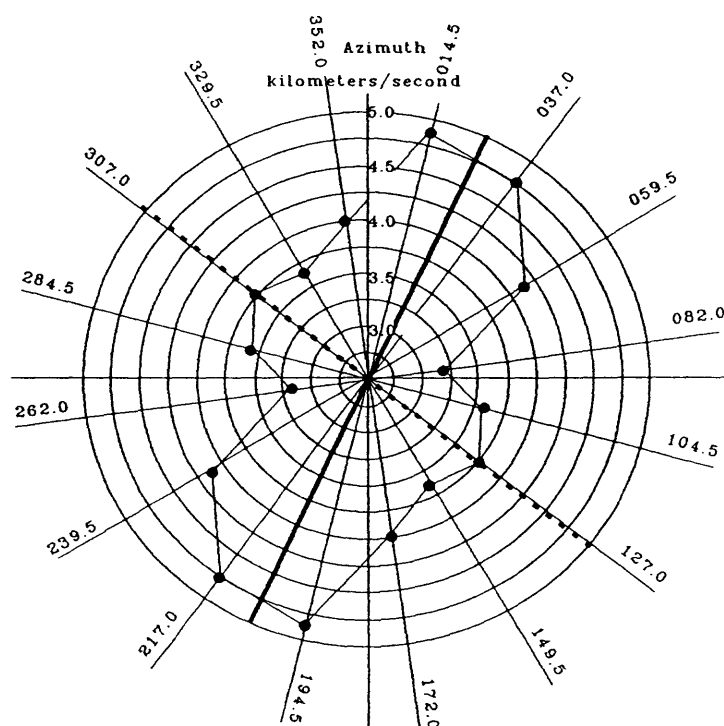
Fig. 9. Seismic compressional wave velocity plotted against azimuth at Priest Field, U.S. Geological Survey fractured bedrock research site, Mirror Lake, New Hampshire. (From Lieblich and others, 1991, fig. 6.)
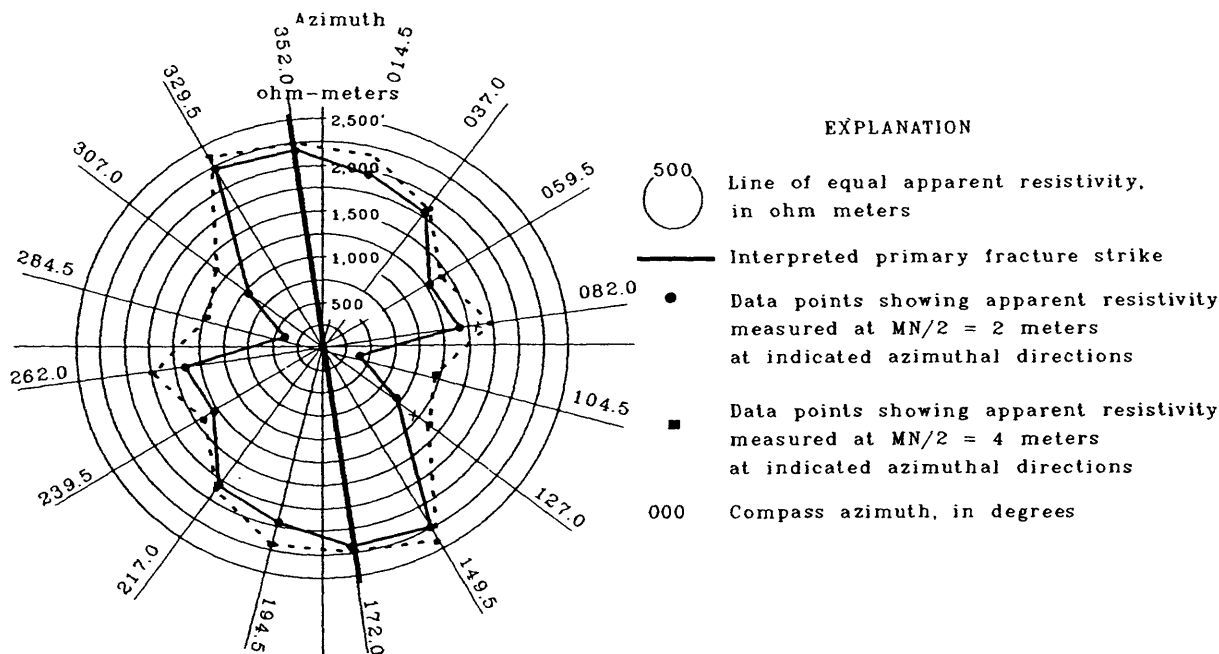
Fig. 10. Schlumberger array apparent resistivity plotted against azimuth for the 40-meter AB/2 spacing, collected at the Camp Osceola well field, U.S. Geological Survey fractured bedrock research site, Mirror Lake, New Hampshire. (From Haeni et al., 1993, fig. 4.)

Azimuthal dc-resistivity methods are sensitive to a sloping bedrock interface (Habberjam, 1975), and a reliable method of correcting for the slope is not available. Results from seismic-refraction surveys at Priest Field indicate that the bedrock surface slopes at less than 5° (D. A. Lieblich, U.S. Geological Survey, oral commun., 1992). This should have a minimal effect on the anisotropy measurement and the interpreted secondary porosity.

Summary

The square-array dc-resistivity method was used to determine the orientation of bedrock fractures at the USGS bedrock research site in the Mirror Lake watershed of the Hubbard Brook Experimental Forest in Grafton County, New Hampshire. A primary fracture strike orientation of 030° was interpreted from a graphical analysis of square-array data and an orientation of 027° was interpreted from
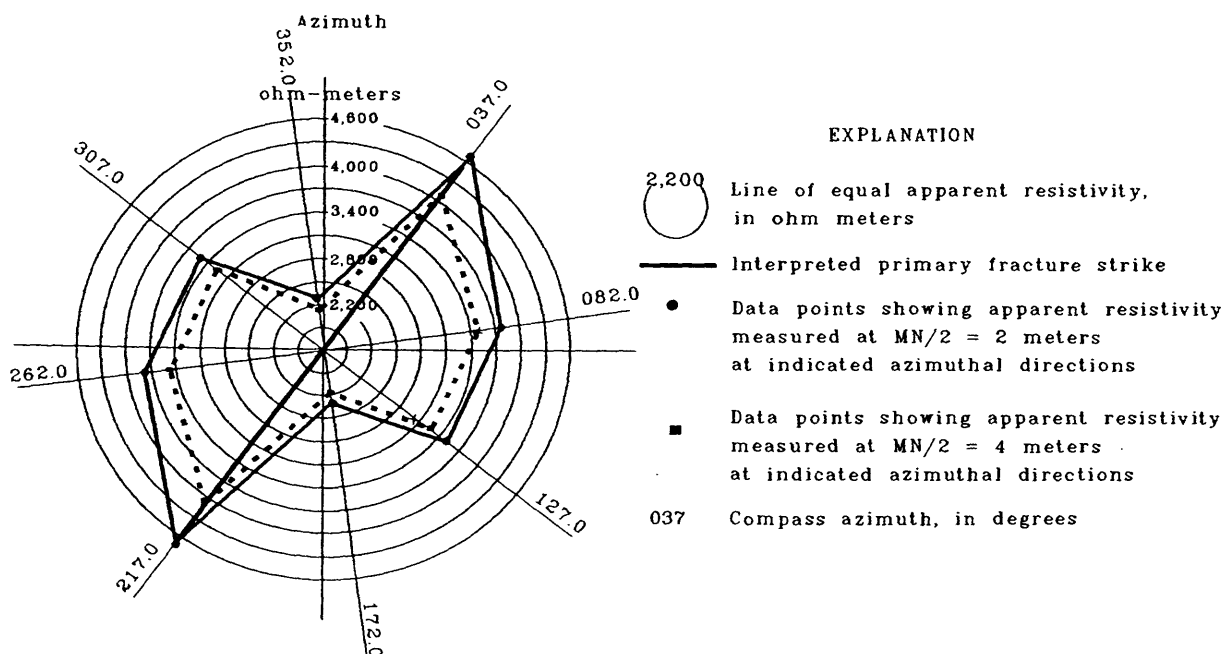

Fig. 11. Schlumberger array apparent resistivity plotted against azimuth for the 40-meter AB/2 spacing, collected at Priest Field, U.S. Geological Survey fractured bedrock research site, Mirror Lake, New Hampshire.

484

47

the analysis of the crossed square-array data. These values closely match the orientation of fracture trends mapped in bedrock (030°) near the sites of surface-geophysical surveys. Fracture-strike orientation interpreted from square-array data is supported by other geophysical data, including azimuthal p-wave seismic refraction (022.5°) and azimuthal Schlumberger dc-resistivity (037° at Camp Osceola). The estimated secondary porosity attributed to fracturing ranged from 0.01 to 0.10, which was higher than the porosity estimated at well CO-1 (0.001). Further comparison of secondary porosity estimates determined from square-array surveys with porosities determined from other sources is needed to assess the square-array secondary porosity calculations.

References

Darboux-Afouda, R. and P. Louis. 1989. Contribution des mesures de l'anisotropic electrique la recherche des aquifres de fracture en milieu cristallin au Benin. Geophysical Prospecting. v. 37, pp. 91-105.

Freeze, R. A. and J. A. Cherry. 1979. Groundwater. Prentice-Hall Inc., Englewood Cliffs, NJ. 604 pp.

Habberjam, G. M. 1972. The effects of anisotropy on square array resistivity measurements. Geophysical Prospecting. v. 20, pp. 249-266.

Habberjam, G. M. 1975. Apparent resistivity, anisotropy and strike measurements. Geophysical Prospecting. v. 23, pp. 211-247.

Habberjam, G. M. 1979. Apparent resistivity observations and the use of square array techniques. In: Saxov, S. and H. Flathe (eds.). Geoexploration Monographs. series 1, no. 9, pp. 1-152.

Habberjam, G. M. and G. E. Watkins. 1967. The use of a square configuration in resistivity prospecting. Geophysical Prospecting. v. 15, pp. 221-235.

Haeni, F. P., J. W. Lane, Jr., and D. A. Lieblich. 1993. Use of surface-geophysical and borehole-radar methods to detect fractures in crystalline rocks, Mirror Lake area, Grafton County, New Hampshire. In: Banks, Sheila and David Banks (eds.). Hydrogeology of Hard Rocks, Memoires of the XXIVth Congress, Oslo, Norway. June 28 to July 2, 1993. Oslo, International Assoc. of Hydrologists. pp. 577-587.

Keller, G. V. and F. C. Frischknecht. 1966. Electrical Methods in Geophysical Prospecting. Pergamon Press, London. 519 pp.

LeMasne, G. 1979. Applications de methodes electriques et electromagnetiques l'etude geophysique des milieus fissures. These 3eme cycle. USTIL Montpelier.

Leonard-Mayer, P. J. 1984a. A surface resistivity method for measuring hydrologic characteristics of jointed formations. U.S. Bureau of Mines Report of Investigations 8901. 45 pp.

Leonard-Mayer, P. J. 1984b. Development and use of azimuthal resistivity surveys for jointed formations. In: Nielsen, D. M. and Mary Curl (eds.). National Water Well Assoc./U.S. Environmental Protection Agency Conference on Surface and Borehole Geophysical Methods in Ground-Water Investigations, San Antonio, TX, Proceedings. National Water Well Assoc., Worthington, OH. pp. 52-91.

Lewis, M. R. and F. P. Haeni. 1987. The use of surface geophysical techniques to detect fractures in bedrock—An annotated bibliography. U.S. Geological Survey Circular 987. 14 pp.

Lieblich, D. A., F. P. Haeni, and R. E. Cromwell. 1992. Integrated use of surface-geophysical methods to indicate subsurface fractures at Tibbetts Road, Barrington, New Hampshire. U.S. Geological Survey Water-Resources Investigations Report 92-4012. 33 pp.

Lieblich, D. A., J. W. Lane, Jr., and F. P. Haeni. 1991. Results of integrated surface-geophysical studies for shallow subsurface fracture detection at three New Hampshire sites. In: Expanded Abstracts with Biographies. SEG 61st Annual International Meeting, Houston, TX, November 10-14, 1991. Society of Exploration Geophysicists, Houston, TX. pp. 553-556.

Mallik, S. B., D. C. Bhattacharya, and S. K. Nag. 1983. Behaviour of fractures in hard rocks—A study by surface geology and radial VES method. Geoexploration. v. 21, pp. 181-189.

McDowell, P. W. 1979. Geophysical mapping of water filled fracture zones in rocks. International Assoc. of Engineering Geology Bulletin. v. 19, pp. 258-264.

Ogden, A. E. and P. S. Eddy, Jr. 1984. The use of tri-potential resistivity to locate fractures, faults and caves for siting high yield water wells. In: Nielsen, D. M. and Mary Curl (eds.). National Water Well Assoc./U.S. Environmental Protection Agency Conference on Surface and Borehole Geophysical Methods in Ground-Water Investigations, San Antonio, TX, Proceedings. National Water Well Assoc., Worthington, OH. pp. 130-149.

Palacky, G. J., I. L. Ritsema, and S. J. De Jong. 1981. Electromagnetic prospecting for groundwater in Precambrian terrains in the Republic of Upper Volta. Geophysical Prospecting. v. 29, pp. 932-955.

Risk, G. F. 1975. Detection of buried zones of fissured rock in geothermal fields using resistivity anisotropy measurements. In: Geophysical papers submitted to the Second U.N. Symposium on the Development and Use of Geothermal Resources, San Francisco, CA, May 20-29. pp. 78-100.

Ritzi, R. W. and R. H. Andolsek. 1992. Relation between anisotropic transmissivity and azimuthal resistivity surveys in shallow fractured carbonate flow systems. Ground Water. v. 30, no. 5, pp. 774-780.

Sauck, W. A. and S. M. Zabik. 1992. Azimuthal resistivity techniques and the directional variations of hydraulic conductivity in glacial sediments. In: Bell, R. S. (ed.). Symposium on the Application of Geophysics to Engineering and Environmental Problems, Oakbrook, IL, April 26-29, 1992, Proceedings. Society of Engineering and Mineral Exploration Geophysicists, Golden, CO. pp. 197-222.

Sehli, A. S. 1990. Contribution of electrical prospecting to the geophysical study of discontinuous media. In: International Symposium on Applications of Geophysics to Water Prospecting in Arid and Semi-Arid Areas, Paris, France.

Soonawala, N. M. and M. R. Dence. 1981. Geophysics in the Canadian nuclear waste program—A case history. Society of Exploration Geophysicists Annual International Meeting, 51st, Los Angeles, CA, 1981, Proceedings. pp. 83-98.

Taylor, R. W. 1982. Evaluation of geophysical surface methods for measuring hydrological variables in fractured rock units. U.S. Bureau of Mines Research Contract Report, contract H0318044. 147 pp.

Taylor, R. W. 1984. The determination of joint orientation and porosity from azimuthal resistivity measurements. In: Nielsen, D. M. and Mary Curl (eds.). National Water Well Assoc./U.S. Environmental Protection Agency Conference on Surface and Borehole Geophysical Methods in Ground-Water Investigations, San Antonio, TX, Proceedings. National Water Well Assoc., Worthington, OH. pp. 37-49.

Taylor, R. W. and A. H. Fleming. 1988. Characterizing jointed systems by azimuthal resistivity surveys. Ground Water. v. 26, no. 4, pp. 464-474.